

# Phase Diagram of an Integrable Alternating $U_q[sl(2|1)]$ Superspin Chain

Holger Frahm<sup>1</sup> and Márcio J. Martins<sup>2</sup>

<sup>1</sup>*Institut für Theoretische Physik, Leibniz Universität Hannover,  
Appelstraße 2, 30167 Hannover, Germany*

<sup>2</sup>*Departamento de Física, Universidade Federal de São Carlos,  
C.P. 676, 13565-905 São Carlos (SP), Brazil*

(Dated: 21. February 2012)

We construct a family of integrable vertex model based on the typical four-dimensional representations of the quantum group deformation of the Lie superalgebra  $sl(2|1)$ . Upon alternation of such a representation with its dual this model gives rise to a mixed superspin Hamiltonian with local interactions depending on the representation parameter  $\pm b$  and the deformation parameter  $\gamma$ . As a subsector this model contains integrable vertex models with ordinary symmetries for twisted boundary conditions. The thermodynamic limit and low energy properties of the mixed superspin chain are studied using a combination of analytical and numerical methods. Based on these results we identify the phases realized in this system as a function of the parameters  $b$  and  $\gamma$ . The different phases are characterized by the operator content of the corresponding critical theory. Only part of the spectrum of this effective theory can be understood in terms of the  $U(1)$  symmetries related to the physical degrees of freedom corresponding to spin and charge. The other modes lead to logarithmic finite-size corrections in the spectrum of the theory.

## I. INTRODUCTION

Integrable quantum spin chains have long been a source of examples of systems presenting rich critical behavior. The critical properties of quantum spin chains based on simply laced Lie algebras are believed to be in the universality class of Wess-Zumino-Witten models on the corresponding group [1, 2]. By way of contrast, the critical behavior of integrable spin chains with both fermionic and bosonic degrees of freedom involves a more subtle understanding. For instance, while superspin chains invariant by the orthosymplectic  $osp(n|2m)$  symmetry are conformally invariant [3] those based on the  $sl(n|m)$  superalgebra appears to be not even relativistic [4]. In addition, the conformal properties of the the spin chain with  $osp(3|2)$  invariance was observed to be unusual thanks to the presence of excitations with zero conformal weight [3]. This type of behaviour has subsequently been seen in the case of the a  $sl(2|1)$  superspin chain that alternates fundamental and dual representations [5]. It was further noted that such degeneracy to the ground state is dominated by a rather remarkable logarithmic finite-size corrections. This peculiar finite-size behaviour has been recently well elaborated from a numerical perspective in the context of a staggered six-vertex model [6]. Here we shall argued that this model hides a twisted quantum group algebra and its integrability can indeed be understood in terms of bosonic and fermionic degrees of freedom.

The purpose of this paper is to introduce and investigate an integrable model whose phase diagram presents all the above mentioned features at once. It can certainly be considered the prototype system mixing critical properties of models based on ordinary Lie algebras and superalgebras. The exactly solved lattice system turns out to be the vertex model built up by alternating one of the four dimensional representations of the  $U_q[sl(2|1)]$  superalgebra with its dual. The fact that these representations can be labelled by a complex number  $b$  and  $-b$  leads to a staggered vertex model with a free parameter. Our paper is organized as follows: in the following section we present and solve this alternating lattice model. There we also expose certain underlying spectral properties of this model which turn out to be essential to uncover its many possible critical phases and discuss its relation to other systems studied previously. In Section III it is argued that the model hides integrable models based from ordinary symmetries with twisted boundary conditions. We then begin our analysis of the thermodynamics and critical properties of the supersymmetric vertex model. In Section IV we consider the case of staggering  $0 \leq b < \frac{1}{2}$ . Both in the antiferromagnetic and the ferromagnetic regime the model is found to be in the universality class of the  $U_q[osp(2|2)]$  spin chain with central charge  $c = -1$ , independent of the parameter  $b$ . We continue with the discussion of the critical behaviour of the ferromagnetic model for  $b > \frac{1}{2}$  in Section V. Here the low

energy effective theory contains four gapless modes, two of them can be identified with the physical spin and charge degrees of freedom of the model. Again, we find that the parameter  $b$  is irrelevant in the continuum limit. Finally, we discuss the thermodynamical limit of the antiferromagnetic model: in Section VI the behaviour for a special choice of the representation parameter satisfying a self-duality condition is analyzed. The operator content is found to be similar to that of the ferromagnetic model. The paper ends with a summary and discussion of our results.

## II. THE MIXED $U_q[sl(2|1)]$ VERTEX MODEL

The four dimensional typical representation of the Lie superalgebra  $sl(2|1)$  has the special feature that the eigenvalues of the azimuthal generator associated to the fermionic degrees of freedom may be any complex number [7]. Therefore, its quantum group deformation  $U_q[sl(2|1)]$  becomes a rich two-parameter algebra and in turn provides a family of solutions of the Yang-Baxter equation [8–10]. We shall denote by  $R_{12}^{(b_1, b_2)}(\lambda)$  the respective  $R$ -matrix acting on the tensor product  $V_1^{(b_1)} \otimes V_2^{(b_2)}$  of two such different four dimensional spaces. The upper labels emphasize the dependence of the  $R$ -matrix on the extra complex variables  $b_1$  and  $b_2$  while  $\lambda$  is the usual spectral parameter. The general structure of the  $R$ -matrix in the symmetrical grading  $FBBF$  is given by [11],

$$\mathcal{R}_{12}^{(b_1, b_2)}(\lambda) = \sum_{j=1}^4 a_j e_{j,j}^{(1)} \otimes e_{j,j}^{(2)} + \sum_{\substack{j,k=1 \\ j \neq k, 5-k}}^4 b_{jk} e_{j,j}^{(1)} \otimes e_{k,k}^{(2)} + \sum_{\substack{j,k=1 \\ j \neq k, 5-k}}^4 c_{jk} e_{j,k}^{(1)} \otimes e_{k,j}^{(2)} + \sum_{j,k=1}^4 d_{jk} e_{5-j,k}^{(1)} \otimes e_{j,5-k}^{(2)} \quad (2.1)$$

where  $e_{j,k}^{(a)} \in \text{End}(\mathbb{C}_a^4)$  are the standard  $4 \times 4$  Weyl matrices. The explicit expressions for the Boltzmann weights  $a_j$ ,  $b_{jk}$ ,  $c_{jk}$  and  $d_{jk}$  are presented in Appendix A.

The above  $R$ -matrix satisfies the Yang-Baxter relation for any three general distinct spaces  $V_1^{(b_1)}$ ,  $V_2^{(b_2)}$  and  $V_3^{(b_3)}$ , namely

$$R_{12}^{(b_1, b_2)}(\lambda) R_{13}^{(b_1, b_3)}(\lambda + \mu) R_{23}^{(b_2, b_3)}(\mu) = R_{23}^{(b_2, b_3)}(\mu) R_{13}^{(b_1, b_3)}(\lambda + \mu) R_{12}^{(b_1, b_2)}(\lambda), \quad (2.2)$$

Considering the weights expressions (A1) we see that the extra variables  $b_i$  enter the Yang-Baxter equation (2.2) in a similar manner as the spectral parameter however in a non-additive form. An immediate consequence is that in general there are two different types of Lax operators obeying the Yang-Baxter algebra with the same  $R$ -matrix. Within the quantum inverse scattering framework one can explore this freedom and construct mixed integrable vertex model. For example, we can combine the Boltzmann weights  $R_{12}^{(b, b_1)}(\lambda)$  and  $R_{12}^{(b, b_2)}(\lambda)$  in such way that the quantum space

states alternate among the  $b_1$  and  $b_2$  representations while the auxiliary space is remains fixed at  $b$ . A schematic representation of this system on a  $2L \times 2L$  square lattice is depicted in Figure 1.

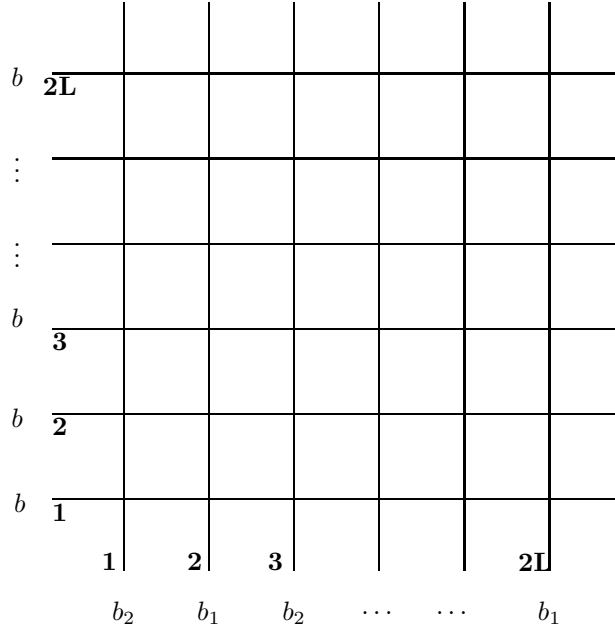


FIG. 1. The mixed vertex with fixed horizontal  $b$  representation.

The row-to-row transfer matrix associated to the mixed vertex model (1) can be formally written as the supertrace [12] over the auxiliary space  $\mathcal{A} \sim V^{(b)}$  of the following ordered product of operators,

$$T^{(b, \{b_1, b_2\})}(\lambda) = \text{Str}_{\mathcal{A}} \left[ \mathcal{R}_{\mathcal{A}, 2L}^{b, b_1}(\lambda) \mathcal{R}_{\mathcal{A}, 2L-1}^{b, b_2}(\lambda) \mathcal{R}_{\mathcal{A}, 2L-2}^{b, b_1}(\lambda) \cdots \mathcal{R}_{\mathcal{A}, 1}^{b, b_2}(\lambda) \right]. \quad (2.3)$$

At this point we recall that due to the Yang-Baxter equations (2.2) the above transfer matrix commutes not only for arbitrary spectral parameters but also for any values of variable  $b$  labeling the horizontal space of states. More precisely the transfer matrix (2.3) satisfies the relation, namely

$$[T^{(b, \{b_1, b_2\})}(\lambda), T^{(\bar{b}, \{b_1, b_2\})}(\mu)] = 0, \quad \forall b, \bar{b} \text{ and } \lambda, \mu. \quad (2.4)$$

The diagonalization of the transfer matrix (2.3) can be carried out within the nested Bethe ansatz framework since  $T^{(b, \{b_1, b_2\})}(\lambda)$  commutes with two distinct  $U(1)$  symmetries. A possible solution is to apply the fusion procedure to obtain a recurrence relation for the eigenvalues of the transfer matrix and combine it with some reasonable analyticity assumptions to fix the corresponding Bethe equations [11, 13, 14]. Yet another method is to explore directly the commutation relations among the monodromy matrix elements in the four dimensional representation. For instance, such constructive approach has been applied to solve the isotropic limit  $q = 1$  of the

plain transfer matrix (2.3) where  $b_1 = b_2 = b$  [15]. Because these methods have been already fully discussed in the literature we shall here present only the final results for the eigenvalues of  $T^{(b, \{b_1, b_2\})}(\lambda)$ . Considering the expressions for the Boltzmann weights (A1) in any of the aforementioned frameworks one can indeed compute the eigenvalues of the transfer matrix (2.3). We find that they can be conveniently written in terms of the product of two terms,

$$\begin{aligned} \Lambda^{(b, \{b_1, b_2\})}(\lambda) &= \left[ -F(\lambda, b, \{\lambda_\ell^{(1)}\}) + \left( \frac{\sinh(\lambda - i\gamma(b - b_1)) \sinh(\lambda - i\gamma(b - b_2))}{\sinh(\lambda - i\gamma(b + b_1 + 1)) \sinh(\lambda - i\gamma(b + b_2 + 1))} \right)^L G(\lambda, b, \{\lambda_\ell^{(1)}\}) \right] \\ &\times \left[ F(\lambda, -b, \{\lambda_\ell^{(2)}\}) - \left( \frac{\sinh(\lambda + i\gamma(b - b_1)) \sinh(\lambda + i\gamma(b - b_2))}{\sinh(\lambda + i\gamma(b + b_1 - 1)) \sinh(\lambda + i\gamma(b + b_2 - 1))} \right)^L G(\lambda, -b, \{\lambda_\ell^{(2)}\}) \right]. \end{aligned} \quad (2.5)$$

The auxiliary functions  $F(\lambda, b, \{\lambda_\ell^{(a)}\})$  and  $G(\lambda, b, \{\lambda_\ell^{(a)}\})$  are given by,

$$\begin{aligned} F(\lambda, b, \{\lambda_\ell^{(a)}\}) &= \prod_{\ell=1}^{N_a} \frac{\sinh(\lambda_\ell^{(a)} - \lambda + i\gamma(b - 1/2))}{\sinh(\lambda_\ell^{(a)} - \lambda - i\gamma(b - 1/2))}, \\ G(\lambda, b, \{\lambda_\ell^{(a)}\}) &= \prod_{\ell=1}^{N_a} \frac{\sinh(\lambda - \lambda_\ell^{(a)} - i\gamma(b + 3/2))}{\sinh(\lambda - \lambda_\ell^{(a)} + i\gamma(b - 1/2))}. \end{aligned} \quad (2.6)$$

while the set of rapidities  $\lambda_j^{(1)}$  and  $\lambda_j^{(2)}$  are required to fulfill the following nested Bethe equations,

$$\begin{aligned} \left\{ \frac{\sinh(\lambda_j^{(1)} + i\gamma(b_1 - \frac{1}{2}))}{\sinh(\lambda_j^{(1)} - i\gamma(b_1 - \frac{1}{2}))} \frac{\sinh(\lambda_j^{(1)} + i\gamma(b_2 - \frac{1}{2}))}{\sinh(\lambda_j^{(1)} - i\gamma(b_2 - \frac{1}{2}))} \right\}^L &= \prod_{k=1}^{N_2} \frac{\sinh(\lambda_j^{(1)} - \lambda_k^{(2)} - i\gamma)}{\sinh(\lambda_j^{(1)} - \lambda_k^{(2)} + i\gamma)}, \quad j = 1, \dots, N_1, \\ \left\{ \frac{\sinh(\lambda_j^{(2)} - i\gamma(b_1 + \frac{1}{2}))}{\sinh(\lambda_j^{(2)} + i\gamma(b_1 + \frac{1}{2}))} \frac{\sinh(\lambda_j^{(2)} - i\gamma(b_2 + \frac{1}{2}))}{\sinh(\lambda_j^{(2)} + i\gamma(b_2 + \frac{1}{2}))} \right\}^L &= \prod_{k=1}^{N_1} \frac{\sinh(\lambda_j^{(2)} - \lambda_k^{(1)} - i\gamma)}{\sinh(\lambda_j^{(2)} - \lambda_k^{(1)} + i\gamma)}, \quad j = 1, \dots, N_2. \end{aligned} \quad (2.7)$$

We stress that the numbers  $N_a$  of Bethe roots are directly related to the two  $U(1)$  symmetries of the model. They determine the eigenvalues of the  $U_q[sl(2|1)]$  charge  $B$  and spin-projection  $S_3$  for the corresponding Bethe state which are  $B = (N_1 - N_2)/2$  and  $S_3 = L - (N_1 + N_2)/2$ . We also observe that the Bethe equations depend only on the alternating representations  $b_1$  and  $b_2$  of the quantum spaces.

In addition, we can use the commuting property (2.4) to built up mixed vertex models with alternation in both horizontal and vertical spaces of states. Of particular interest are those whose transfer matrix commutes with one-dimensional spin Hamiltonians possessing a finite number of local interactions for any size  $L$ . The simplest such case occurs when we alternate between a given representation  $b$  and its dual counterpart  $-b$ . In Figure 2 we exhibit the graphical representation of this type of double mixed vertex model. The corresponding transfer matrix is given in terms of

the following product of commuting operators,

$$T^{(mix)}(\lambda) = T^{(b, \{b, -b\})}(\lambda) T^{(-b, \{b, -b\})}(\lambda). \quad (2.8)$$

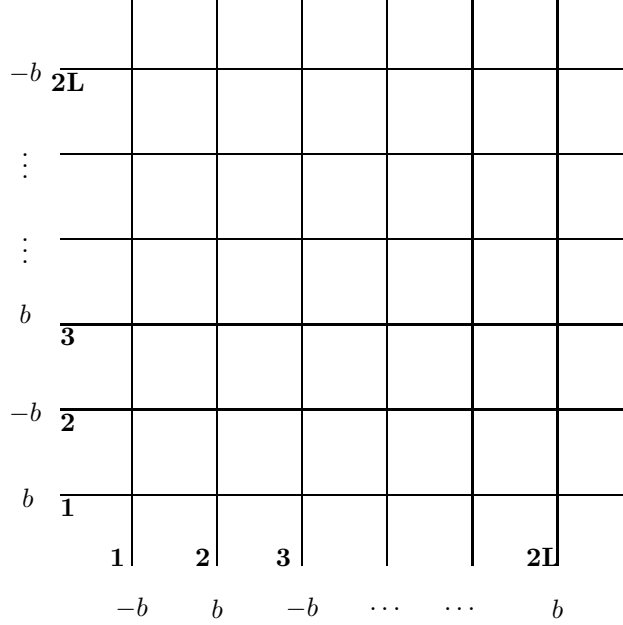


FIG. 2. The mixed vertex with alternation  $\pm b$  in both horizontal and vertical spaces.

Because we are dealing with a family of commuting operators the eigenvalues of the transfer matrix  $T^{(mix)}(\lambda)$  is just the product of the individual eigenvalues,

$$\Lambda^{(mix)}(\lambda) = \Lambda^{(b, \{b, -b\})}(\lambda) \Lambda^{(-b, \{b, -b\})}(\lambda) \quad (2.9)$$

where  $\Lambda^{(\pm b, \{b, -b\})}(\lambda)$  are easily computed from Eqs.(2.5) and (2.6).

By the same token, the corresponding Bethe equations are obtained from Eqs.(2.7) by substituting  $b_1 = b$  and  $b_2 = -b$ . We note that for this choice of alternation the Bethe equations (2.7) turn out to be invariant under the change of the sign of the parameter  $b$ . Since we will be referring to these equations in many distinct circumstances on the paper we for sake of clarity shall quote them explicitly

$$\left\{ \frac{\sinh(\lambda_j^{(1)} + i\gamma(b - \frac{1}{2}))}{\sinh(\lambda_j^{(1)} - i\gamma(b - \frac{1}{2}))} \frac{\sinh(\lambda_j^{(1)} - i\gamma(b + \frac{1}{2}))}{\sinh(\lambda_j^{(1)} + i\gamma(b + \frac{1}{2}))} \right\}^L = \prod_{k=1}^{N_2} \frac{\sinh(\lambda_j^{(1)} - \lambda_k^{(2)} - i\gamma)}{\sinh(\lambda_j^{(1)} - \lambda_k^{(2)} + i\gamma)}, \quad j = 1, \dots, N_1, \\ \left\{ \frac{\sinh(\lambda_j^{(2)} + i\gamma(b - \frac{1}{2}))}{\sinh(\lambda_j^{(2)} - i\gamma(b - \frac{1}{2}))} \frac{\sinh(\lambda_j^{(2)} - i\gamma(b + \frac{1}{2}))}{\sinh(\lambda_j^{(2)} + i\gamma(b + \frac{1}{2}))} \right\}^L = \prod_{k=1}^{N_1} \frac{\sinh(\lambda_j^{(2)} - \lambda_k^{(1)} - i\gamma)}{\sinh(\lambda_j^{(2)} - \lambda_k^{(1)} + i\gamma)}, \quad j = 1, \dots, N_2. \quad (2.10)$$

We now observe that for  $\lambda = 0$  both  $\mathcal{R}_{12}^{b,b}(\lambda)$  and  $\mathcal{R}_{12}^{-b,-b}(\lambda)$  turn out to be the graded permutator and  $T^{(mix)}(\lambda = 0)$  become proportional to the two-sites translation operator. The respective local spin chain Hamiltonian is then constructed by taking the logarithmic derivative of the transfer matrix (2.8) at  $\lambda = 0$ , namely

$$\mathcal{H}^{(mix)} = i \frac{\partial}{\partial \lambda} \ln T^{(mix)}(\lambda) \Big|_{\lambda=0}. \quad (2.11)$$

The operator (2.11) defines an integrable superspin Hamiltonian with local two- and three-spin interactions. Considering Eqs. (2.5), (2.9) we find that the eigenspectrum of  $H^{(mix)}$  in a given sector  $N_1$  and  $N_2$  is parameterized by the following expression

$$E_{N_1, N_2}^{(mix)}(b, \gamma) = \sum_{a=1,2} \sum_{\ell=1}^{N_a} \left\{ \frac{2 \sin(\gamma(2b+1))}{\cos(\gamma(2b+1)) - \cosh 2\lambda_{\ell}^{(a)}} - \frac{2 \sin(\gamma(2b-1))}{\cos(\gamma(2b-1)) - \cosh 2\lambda_{\ell}^{(a)}} \right\}. \quad (2.12)$$

where  $\{\lambda_{\ell}^{(a)}\}$ ,  $a = 1, 2$  are solutions of the Bethe equations (2.10).

We now discuss some properties concerning the eigenspectrum (2.10) and (2.12) of the superspin chain which will be helpful in the analysis of the thermodynamic limit behavior. We first note that the spectrum of this model remains unchanged under the replacements  $2\gamma b \rightarrow \pi - 2\gamma b$  and  $\lambda_j^{(a)} \rightarrow \lambda_j^{(a)} + i\pi/2$ . In other words we have a remarkable spectral relation for two distinct values of  $b$ ,

$$E_{N_1, N_2}^{(mix)}(b, \gamma) = E_{N_1, N_2}^{(mix)}(\pi/(2\gamma) - b, \gamma). \quad (2.13)$$

The identity (2.13) allows to restrict our study of the complete phase diagram of the mixed superspin chain to the region  $0 < \gamma b \leq \pi/4$  for a given value of the anisotropy  $\gamma$  lying in the regime  $0 < \gamma \leq \pi$ . From (2.13) we also see that the line  $b\gamma = \pi/4$  is rather special since the spectrum is mapped onto itself. This implies that the individual Bethe roots remain invariant under the shift  $\lambda_j^{(a)} \rightarrow \lambda_j^{(a)} + i\pi/2$  which reflects the presence of some discrete  $\mathbf{Z}_2$  invariance of the model on this line which we denote as 'self-dual line' of the model in the following. We note here that a similar fact has been observed before for a particular staggered six-vertex model [6].

Furthermore, as is typical of spin chains derived from quantum group algebras, one also expects that spectrum of  $\mathcal{H}^{(mix)}$  at  $\gamma$  and  $\pi - \gamma$  should be related to each other. Direct inspection of Eqs. (2.10) and (2.12) reveals this relation to be

$$E_{N_1, N_2}^{(mix)}(b, \gamma) = -E_{N_1, N_2}^{(mix)}(\gamma b/(\pi - \gamma), \pi - \gamma) \quad (2.14)$$

From Eq.(2.14) we conclude that the spectrum of  $H^{(mix)}$  changes sign under the replacement  $\gamma \rightarrow \pi - \gamma$  while leaving the product  $b\gamma$  unchanged. This symmetry is useful to study both

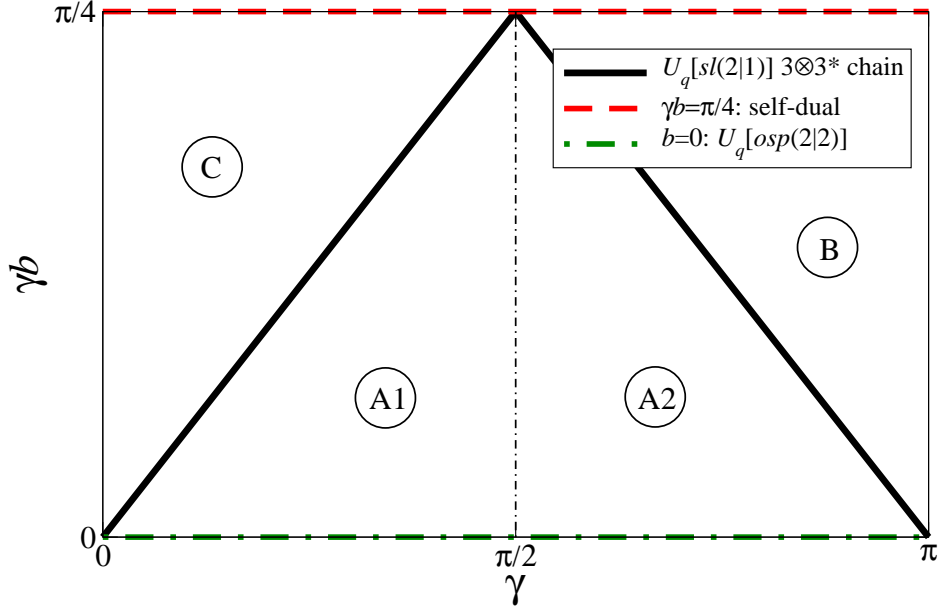


FIG. 3. Parameter space of the mixed superspin chain.

the antiferromagnetic mixed superspin chain (2.11) and the ferromagnetic one with Hamiltonian  $-\mathcal{H}^{(mix)}$  while considering the deformation parameter on the region  $0 < \gamma \leq \pi/2$ .

In Figure 3 we summarize the region of parameters space one should concentrate the analysis of the physical properties.

It turns out that for certain choices of the representation parameter  $b$  the mixed superspin model introduced above has been already studied in the literature. In what follows we summarize the main previous results on this system:

- For  $b = 0$  the alternating representations are the same and we have a homogeneous vertex model and a corresponding spin chain with only two-body interactions. We see that the Bethe equations (2.10) and the expressions (2.12) for the eigenvalues simplify drastically. In Ref. 16 the critical properties of the corresponding *antiferromagnetic*  $U_q[osp(2|2)]$  superspin chain have been studied. The continuum theory was found to have central charge  $c = -1$  with dimensions varying continuously with the deformation parameter  $\gamma$ .
- For  $b = \pm \frac{1}{2}$  the four-dimensional representations used for the construction of the mixed superspin model (2.8) degenerate into the *atypical* three-dimensional ones,  $3$  and  $\bar{3}$ , see also the discussion in Appendix B. The continuum model describing the low energy behaviour of the *antiferromagnetic*  $3 \otimes \bar{3}$ -superspin chain has been identified as a  $c = 0$  theory for  $\gamma < \pi/4$



[5, 17].<sup>1</sup> The operator content has been attributed to one compact and one non-compact bosonic degree of freedom. Both the compactification radius of the former and the spectral fine structure due to the latter depend on the deformation parameter  $\gamma$ .

For *ferromagnetic* exchange the spectrum of low-lying states of the  $3 \otimes \bar{3}$ -superspin chain have been found to be the same as for the  $U_q[osp(2|2)]$  with central charge  $c = -1$ . The scaling dimensions of this model exhibit exact spin charge separation, the excitations in both sectors are free bosons with compactification radii depending on  $\gamma$ . In the isotropic limit,  $\gamma \rightarrow 0$ , the magnetic part of the spectrum turns non-relativistic.

Considering the above informations we see that the phase diagram Fig. 3 has been only marginally investigated so far. In this paper we provide results on the thermodynamics and critical properties of the superspin chain which allow to characterize the model throughout its parameter space. Specifically, we shall investigate the model the four regions

- phase A1: the antiferromagnetic superspin chain for  $b < \frac{1}{2}$ ,
- phase A2: the ferromagnetic superspin chain for  $b < \frac{1}{2}$ ,
- phase B: the antiferromagnetic superspin chain for  $\frac{1}{2} < b \leq \pi/4\gamma$ .
- phase C: the antiferromagnetic superspin chain for  $\frac{1}{2} < b \leq \pi/4\gamma$ , and

Before turning to this problem let us first discuss another important feature of the alternating vertex model (2.8) that will be useful in the analysis of its physical properties. It turns out that this model hides integrable systems based on ordinary symmetries with suitable twisted boundary conditions. We detail this property in next section.

### III. HIDDEN STAGGERED SIX-VERTEX MODELS

The interest in the study of staggered vertex models probably emerged with the work of Temperley and Lieb where a remarkable equivalence between the partition function of a staggered six-vertex model and that of a spin system denominated  $q$ -state Potts model was proposed [18]. This relationship was further elaborated for various types of lattices [19]. In particular it was argued that there exist two manifolds of statistical weights for a staggered six-vertex model which are solvable by Bethe ansatz methods [20]. Nowadays, the quantum inverse scattering framework

---

<sup>1</sup> Note that the parametrization of the deformation in Ref. 17 differs from the one used here by a factor of 2.

[21] provides a general procedure to construct integrable staggered vertex models from solutions of the Yang-Baxter equation. Typical examples are models whose transfer matrix are built up by staggering the spectral parameters of an additive  $R$ -matrix between two or more different values.

In what follows we shall argue that there is a one-to-one correspondence between part of the spectrum of the mixed  $U_q[sl(2|1)]$  vertex model and the eigenvalues of the transfer matrix  $T_{6v}(\lambda)$  of a staggered six-vertex model with anti-periodic boundary conditions. The latter can be written as the product of commuting single-row transfer matrices

$$T_{6v}(\lambda) = T_{stg}(\lambda)T_{stg}(\lambda + 2ib\gamma) \quad (3.1)$$

where the operator  $T_{stg}(\lambda)$  is the transfer matrix constructed from the  $R$ -matrix of the six-vertex model in which the spectral parameters alternates between  $\lambda$  and  $\lambda - 2ib\gamma$ . The expression for  $T_{stg}(\lambda)$  is therefore given by

$$T_{stg}(\lambda) = Tr_{\mathcal{A}} \left[ G_{\mathcal{A}} \mathcal{R}_{\mathcal{A}2L}^{(6v)}(\lambda) \mathcal{R}_{\mathcal{A}2L-1}^{(6v)}(\lambda - 2ib\gamma) \mathcal{R}_{\mathcal{A}2L-1}^{(6v)}(\lambda) \cdots \mathcal{R}_{\mathcal{A}1}^{(6v)}(\lambda - 2ib\gamma) \right], \quad (3.2)$$

with the standard  $R$ -matrix associated to the symmetrical six-vertex model

$$\mathcal{R}^{(6v)}(\lambda) = \begin{pmatrix} 1 & 0 & 0 & 0 \\ 0 & \frac{\sinh(\lambda)}{\sinh(\lambda-i\gamma)} & \frac{\sinh(-i\gamma)}{\sinh(\lambda-i\gamma)} & 0 \\ 0 & \frac{\sinh(-i\gamma)}{\sinh(\lambda-i\gamma)} & \frac{\sinh(\lambda)}{\sinh(\lambda-i\gamma)} & 0 \\ 0 & 0 & 0 & 1 \end{pmatrix}, \quad (3.3)$$

The matrix  $G_{\mathcal{A}}$  in (3.2) encodes the freedom of choices of toroidal boundary conditions compatible with integrability. Here we assume that it preserves the bulk  $U(1)$  symmetry and therefore is diagonal,

$$G_{\mathcal{A}} = \begin{pmatrix} 1 & 0 \\ 0 & e^{i\varphi} \end{pmatrix}, \quad 0 \leq \varphi \leq \pi. \quad (3.4)$$

The transfer matrix (3.2) with boundary condition (3.4) can be diagonalized by applying the so-called  $ABCD$  algebraic Bethe ansatz method [21]. Since this framework has been well discussed in the literature, see for instance [22], we shall present only the main results that are of interest here. The underlying  $U(1)$  invariance implies that the Hilbert space can be split into disjoint sectors labeled by the eigenvalues of the total azimuthal magnetization operator  $S_3 = \frac{1}{2} \sum_{j=1}^{2L} \sigma_j^z$ . The corresponding eigenvalues  $\Lambda_N(\lambda, \varphi)$  of  $T_{stg}(\lambda)$  in the sector with magnetization  $L - N$  where

$N = 0, \dots, L$  are given by,

$$\Lambda_N(\lambda, \varphi; \{\lambda_j\}) = \prod_{j=1}^N \frac{\sinh(\lambda_j - \lambda - i\gamma/2)}{\sinh(\lambda_j - \lambda + i\gamma/2)} + e^{i\varphi} \left[ \frac{\sinh(\lambda - i2b\gamma) \sinh(\lambda)}{\sinh(\lambda - i\gamma) \sinh(\lambda - i\gamma - i2b\gamma)} \right]^L \prod_{j=1}^N \frac{\sinh(\lambda - \lambda_j - i3\gamma/2)}{\sinh(\lambda - \lambda_j - i\gamma/2)}. \quad (3.5)$$

The eigenstates are parameterized by the rapidities  $\lambda_j$  which satisfy the following Bethe ansatz equations,

$$\left[ \frac{\sinh(\lambda_j - i\gamma/2) \sinh(\lambda_j - i\gamma/2 - i2b\gamma)}{\sinh(\lambda_j + i\gamma/2) \sinh(\lambda_j + i\gamma/2 - i2b\gamma)} \right]^L = e^{i\varphi} \prod_{\substack{k=1 \\ k \neq j}}^N \frac{\sinh(\lambda_j - \lambda_k - i\gamma)}{\sinh(\lambda_j - \lambda_k + i\gamma)}, \quad j = 1, \dots, N. \quad (3.6)$$

Using (3.1) the transfer matrix eigenvalues  $\Lambda_N^{(6v)}(\lambda, \varphi)$  of the staggered six vertex model can be written a product of two terms, namely

$$\Lambda_N^{(6v)}(\lambda, \varphi; \{\lambda_j\}) = \Lambda_N(\lambda, \varphi; \{\lambda_j\}) \Lambda_N(\lambda + i2b\gamma, \varphi; \{\lambda_j\}) \quad (3.7)$$

We have now the main ingredients to identify part of the spectrum of the mixed transfer matrix (2.8) with the eigenvalues of the staggered six-vertex model with anti-periodic boundary condition  $\varphi = \pi$ : Facilitated by their symmetrical form the Bethe equations (2.10) allow for solutions in the zero charge sector ( $N_1 = N_2 = N$ ) with coinciding roots, i.e.  $\{\lambda_j^{(1)}\} \equiv \{\lambda_j^{(2)}\}$ . Under these conditions is not difficult to see that Bethe ansatz equations (2.10) of the mixed  $U_q[sl(2|1)]$  vertex model coincide with those associated to the staggered six-vertex model (3.6) after the identification  $\lambda_j = \lambda_j^{(1)} + ib\gamma$ . Furthermore, by expanding the products entering in Eq.(2.9) and comparing them with that given by expressions (3.5), (3.7) one is able to see the following direct correspondence,

$$\Lambda_{N,N}^{(mix)}(\lambda; \{\lambda_j^{(1)}\}, \{\lambda_j^{(1)}\}) \equiv \Lambda_N^{(6v)}(\lambda, \varphi = \pi; \{\lambda_j^{(1)} + ib\gamma\}) \quad (3.8)$$

where the rapidities are now solutions of

$$\left[ \frac{\sinh(\lambda_j^{(1)} + ib\gamma - i\gamma/2) \sinh(\lambda_j^{(1)} - ib\gamma - i\gamma/2)}{\sinh(\lambda_j^{(1)} + ib\gamma + i\gamma/2) \sinh(\lambda_j^{(1)} - ib\gamma + i\gamma/2)} \right]^L = - \prod_{\substack{k=1 \\ k \neq j}}^N \frac{\sinh(\lambda_j^{(1)} - \lambda_k^{(1)} - i\gamma)}{\sinh(\lambda_j^{(1)} - \lambda_k^{(1)} + i\gamma)}, \quad j = 1, \dots, N. \quad (3.9)$$

As a consequence of (3.8) the corresponding energy eigenvalues (2.12) of the  $U_q[sl(2|1)]$  superspin chain are related to those of the spin chain associated to the staggered six-vertex model by

$$E_{N,N}^{(mix)} = 2E_N^{(6v)}(\varphi = \pi) \quad (3.10)$$

where

$$E_N^{(6v)}(\varphi) = i \left. \frac{\partial}{\partial \lambda} \ln \Lambda_N^{(6v)}(\lambda, \varphi; \{\lambda_j^{(1)} + ib\gamma\}) \right|_{\lambda=0} \quad (3.11)$$

We would like to conclude this section with the following remarks. The staggered six-vertex model has at least two particular lines in which certain quantum group symmetries show up. The first occurs at  $b = 1/2$  in which the  $R$ -matrix (3.3) of the six-vertex model with rapidity  $\lambda = 2i\gamma b$  becomes proportional to a projector. In this case the product of neighbouring  $R$ -matrices in (3.2) behaves much like in the fusion procedure for two spins-1/2 and the underlying quantum symmetry is that present on the integrable XXZ spin-1 chain [23]. The second peculiar line turns out to be again  $\gamma b = \pi/4$  which is equivalent to one of the integrable manifolds of the  $q$ -state Potts model with antiferromagnetic couplings [20]. This equivalence has been recently re-elaborated in Ref. 6 where arguments in favour of a possible underlying quantum group symmetry were given however without any precise proposal. In what follows we shall argue that such an invariance is directly related to the twisted quantum algebra  $U_q[D_2^{(2)}]$  with  $q = e^{2i\gamma}$ . In fact, we are going to show that the transfer matrix spectrum of the staggered six-vertex model on the line  $\gamma b = \pi/4$  is the same as that of the plain  $U_q[D_2^2]$  vertex model with  $L$  sites. In order to do that we start by defining the latter transfer matrix,

$$T_{D_2^2}(\lambda) = \text{Tr}_{\mathcal{A}} \left[ \bar{G}_{\mathcal{A}} \mathcal{R}_{\mathcal{A}L}^{(D_2^2)}(\lambda) \mathcal{R}_{\mathcal{A}L-1}^{(D_2^2)}(\lambda) \cdots \mathcal{R}_{\mathcal{A}1}^{(D_2^2)}(\lambda) \right], \quad (3.12)$$

where  $\mathcal{R}_{12}^{(D_2^2)}(\lambda)$  denotes the  $R$ -matrix of the  $U_q[D_2^2]$  vertex model. This is a four state vertex model and the explicitly form of the  $R$ -matrix can be found in the original work by Jimbo [24].

The toroidal boundary condition is represented by the  $c$ -number matrix  $\bar{G}_{\mathcal{A}}$ . It turns out that the most general diagonal matrix preserving the commutativity of the transfer matrix (3.12) for different values of the spectral parameter is,

$$\bar{G}_{\mathcal{A}} = \begin{pmatrix} 1 & 0 & 0 & 0 \\ 0 & e^{i\varphi} & 0 & 0 \\ 0 & 0 & e^{i\varphi} & 0 \\ 0 & 0 & 0 & e^{2i\varphi} \end{pmatrix}, \quad 0 \leq \varphi \leq \pi. \quad (3.13)$$

It is possible to find the eigenvalues  $\bar{\Lambda}_N(\lambda, \varphi)$  of the transfer matrix (3.12) by adapting the algebraic diagonalization procedure devised in [25] to include the twisted boundary conditions (3.13). The index  $N$  denotes the many possible  $U(1)$  sectors that are underlying the quantum  $U_q[D_2^2]$  algebra. Following such algebraic approach we find that the eigenvalues of  $T_{D_2^2}(\lambda)$  given in

terms of the Bethe rapidities  $\{\mu_j\}$  can be written as,

$$\begin{aligned} \Lambda_N^{(D_2^2)}(\lambda, \varphi; \{\mu_j\}) &= [R_{11}^{11}(\lambda)]^L \prod_{j=1}^N \frac{R_{11}^{11}(\mu_j - \lambda)}{R_{12}^{12}(\mu_j - \lambda)} + e^{i\varphi} \left[ \frac{R_{12}^{12}(\lambda)}{R_{11}^{11}(\lambda)} \right]^L \Lambda^{(16v)}(\lambda, \{\mu_j\}) \\ &\quad + e^{2i\varphi} \left[ \frac{R_{41}^{41}(\lambda)}{R_{11}^{11}(\lambda)} \right]^L \prod_{j=1}^N \frac{R_{12}^{12}(\lambda - \mu_j)}{R_{41}^{41}(\lambda - \mu_j)} \end{aligned} \quad (3.14)$$

where the elements  $R_{ab}^{cd}$  can be read from the  $U_q[D_2^2]$   $R$ -matrix ([24]) by the relation  $R(\lambda) = \sum_{a,b,c,d=1}^4 R_{ab}^{cd}(\lambda) e_{ac} \otimes e_{bd}$ .

To make a comparison with the eigenvalues of the staggered six-vertex model we shall first normalized the  $R$ -matrix by setting  $R_{11}^{11}(\lambda) = 1$ . The expressions of the other needed  $R$ -matrix elements in Eq. (3.14) can then be easily read from the original work by Jimbo [24]. We next choose the spectral variable  $x$  and the anisotropy  $k$  used in this later work to be  $x = e^{2\lambda}$  and  $k = e^{2i\gamma}$ . Considering these definitions the expressions of the  $R$ -matrix elements entering Eq.(3.14) are,

$$R_{12}^{12}(\lambda) = \frac{\sinh(2\lambda)}{\sinh(2\lambda - 2i\gamma)}, \quad R_{41}^{41}(\lambda) = \left[ \frac{\sinh(2\lambda)}{\sinh(2\lambda - 2i\gamma)} \right]^2 \quad (3.15)$$

The function  $\Lambda^{(16v)}(\lambda, \{\mu_j\})$  corresponds to the eigenvalue of the transfer matrix of an inhomogeneous sixteen-vertex that naturally emerges in the nested algebraic Bethe ansatz formulation. As explained in Ref. 25 such sixteen-vertex model is special and its transfer matrix can be diagonalized without the recourse of a second Bethe ansatz. Considering the results of [25] one finds that the expression for such eigenvalues in our notation is,

$$\Lambda^{(16v)}(\lambda, \{\mu_j\}) = \prod_{j=1}^N \frac{\sinh(2\lambda - 2\mu_j) + \epsilon_j \sinh(2i\gamma)}{\sinh(2\lambda - 2\mu_j)} + \prod_{j=1}^N \frac{\sinh(2\lambda - 2\mu_j) - \epsilon_j \sinh(2i\gamma)}{\sinh(2\lambda - 2\mu_j)} \quad (3.16)$$

where  $\epsilon_j = \pm 1$  is a discrete  $Z_2$  variable entering in the corresponding eigenvectors.

Putting all these results together and after few simplifications we find the the final expression for the eigenvalue  $\Lambda_N^{(D_2^2)}(\lambda, \varphi; \{\mu_j\})$  is given by,

$$\begin{aligned} \Lambda_N^{(D_2^2)}(\lambda, \varphi; \{\mu_j\}) &= \prod_{j=1}^N \frac{\sinh(2\mu_j - 2\lambda - 2i\gamma)}{\sinh(2\mu_j - 2\lambda)} + e^{2i\varphi} \left[ \frac{\sinh(2\lambda)}{\sinh(2\lambda - 2i\gamma)} \right]^{2L} \prod_{j=1}^N \frac{\sinh(2\lambda - 2\mu_j - 2i\gamma)}{\sinh(2\lambda - 2\mu_j)} \\ &\quad + e^{i\varphi} \left[ \frac{\sinh(2\lambda)}{\sinh(2\lambda - 2i\gamma)} \right]^L \left\{ \prod_{j=1}^N \frac{2 \sinh(\lambda - \mu_j - i\gamma) \cosh(\lambda - \mu_j + i\gamma)}{\sinh(2\lambda - 2\mu_j)} \right. \\ &\quad \left. + \prod_{j=1}^N \frac{2 \sinh(\lambda - \mu_j + i\gamma) \cosh(\lambda - \mu_j - i\gamma)}{\sinh(2\lambda - 2\mu_j)} \right\} \end{aligned} \quad (3.17)$$

It is not difficult to see that Eq.(3.17) also factorizes into a product of two terms. By defining  $\mu_j = \lambda_j + i\frac{\gamma}{2}$  we see that such product form is exactly identified with the eigenvalues of the staggered six-vertex model when  $\gamma b = \pi/4$  given by Eqs.(3.5), (3.7).

We finally recall that the  $D_2^2$   $R$ -matrix can be obtained by Baxterizing the dilute Birman-Wenzel-Murakami algebra associated to the  $O(3)$  braid representation [26]. Following Ref. 27 one can also show that such  $R$ -matrix (now graded) can be alternatively be derived by means of the dilute Baxterization of the  $osp(1|2)$  superalgebra. This means that the staggered vertex model for  $\gamma b = \pi/4$  hides both the fermionic and bosonic degrees of freedom. From this observation it follows directly that the isotropic limit  $\gamma \rightarrow \pi/2$  has indeed an  $osp(2|2)$  symmetry as first pointed out in Ref. 28.

#### IV. THERMODYNAMIC LIMIT AND CRITICAL PROPERTIES FOR $0 \leq b < \frac{1}{2}$

We are now going to discuss the thermodynamic limit and the low energy properties of the mixed vertex model (2.8). Our discussion will be based on the identification those root configurations solving the Bethe equations (2.10) which correspond to the low lying eigenstates of (2.11) for given values of the parameters  $b$  and  $\gamma$  as obtained by numerical diagonalization of small systems.

It is well established that in the thermodynamic limit  $L \rightarrow \infty$  the solutions of the Bethe equations (3.9) for the staggered six vertex with  $b \leq \frac{1}{2}$  are generically grouped into 'strings' consisting of  $m$  complex rapidities  $\lambda_{(m),j}$  characterized by a common real center  $\lambda_{(m)}$  and a parity  $v_m = \pm 1$ :

$$\lambda_{(m),j} = \lambda_{(m)} + i\frac{\gamma}{2}(m+1-2j) + i\frac{\pi}{4}(1-v_m), \quad j = 1, \dots, m. \quad (4.1)$$

The allowed values of  $(m, v_m)$  depend on the anisotropy  $\gamma$  in a rather involved way [29]. For the mixed superspin chain the string classification has been done for the case  $b \equiv \frac{1}{2}$  [5, 17]. Away from this line we have to rely on the procedure outlined above. We find that for  $b < \frac{1}{2}$  most of the root configurations solving (2.10) corresponding to the ground state and low energy excitations can be organized into strings of length 1 of both parities:  $(1, +)$ ,  $(1, -)$ .

##### A. Phase A1: Anti-ferromagnetic regime for $0 \leq b < \frac{1}{2}$

Exact diagonalization of the Hamiltonian shows that the ground state of the antiferromagnetic mixed superspin chain for  $b \in [0, \frac{1}{2})$  lies in the sectors  $(N_1, N_2) = (L, L-1)$  and  $(N_1, N_2) = (L-1, L)$  corresponding to charge  $B = \pm \frac{1}{2}$  and spin  $S_3 = \frac{1}{2}$  (the states with  $S_3 = -\frac{1}{2}$  are obtained by application of the global  $\mathbb{Z}_2$ -symmetry of the mixed chain, i.e. reversal of all spins), i.e. fourfold degenerate. Furthermore, we find that these states as well as many low lying excitations can be described by real solutions to the Bethe equations (2.10).

Based on this observation we shall now study this state in the thermodynamic limit  $L \rightarrow \infty$  with  $N_a/L \rightarrow 1$ : taking the logarithm of the Bethe equations (2.10) we obtain

$$\begin{aligned} L \left[ \Phi(\lambda_j^{(1)}, \gamma(b + \frac{1}{2})) - \Phi(\lambda_j^{(1)}, \gamma(b - \frac{1}{2})) \right] &= 2\pi Q_j^{(1)} + \sum_{k=1}^{N_2} \Phi(\lambda_j^{(1)} - \lambda_k^{(2)}, \gamma), \quad j = 1, \dots, N_1 \\ L \left[ \Phi(\lambda_j^{(2)}, \gamma(b + \frac{1}{2})) - \Phi(\lambda_j^{(2)}, \gamma(b - \frac{1}{2})) \right] &= 2\pi Q_j^{(2)} + \sum_{k=1}^{N_1} \Phi(\lambda_j^{(2)} - \lambda_k^{(1)}, \gamma), \quad j = 1, \dots, N_2 \end{aligned} \quad (4.2)$$

with

$$\Phi(x, y) = 2 \arctan(\tanh(x) \cot(y)). \quad (4.3)$$

In (4.2) the numbers  $Q_j^{(a)}$  define the many possible branches of the logarithm. They have to be chosen integer or half-odd integer depending on the parities of  $N_a$  according to the rule

$$Q_j^{(1)} \equiv \frac{N_2}{2} \pmod{1}, \quad Q_j^{(2)} \equiv \frac{N_1}{2} \pmod{1}. \quad (4.4)$$

The root configuration corresponding to the ground state in the sector  $(L, L-1)$  is defined by consecutive values for these quantum numbers, i.e.  $Q_j^{(1)} = -(L-1)/2, -(L-3)/2, \dots, (L-1)/2$  and  $Q_j^{(2)} = -L/2 + 1, -L/2 + 2, \dots, L/2 - 1$ .

#### Thermodynamic limit

Following Yang and Yang [30] we introduce counting functions

$$\begin{aligned} z^{(1)}(\lambda) &= \frac{1}{2} \left( \Phi(\lambda, \gamma(b + \frac{1}{2})) - \Phi(\lambda, \gamma(b - \frac{1}{2})) \right) - \frac{1}{2L} \sum_{k=1}^{N_2} \Phi(\lambda - \lambda_k^{(2)}, \gamma), \\ z^{(2)}(\lambda) &= \frac{1}{2} \left( \Phi(\lambda, \gamma(b + \frac{1}{2})) - \Phi(\lambda, \gamma(b - \frac{1}{2})) \right) - \frac{1}{2L} \sum_{k=1}^{N_1} \Phi(\lambda - \lambda_k^{(1)}, \gamma). \end{aligned} \quad (4.5)$$

By definition, we have  $z^{(a)}(\lambda_j^{(a)}) = \pi Q_j^{(a)}/L$ . In the thermodynamic limit the roots of the Bethe equations fill the entire real axis with densities

$$2\pi\rho^{(a)}(\lambda) = \frac{dz^{(a)}(\lambda)}{d\lambda}, \quad a = 1, 2. \quad (4.6)$$

They satisfy coupled linear integral equations obtained by taking derivatives of Eqs. (4.5)

$$\begin{aligned} \rho^{(1)}(\lambda) &= \frac{1}{4\pi} \left( \Phi'(\lambda, \gamma(b + \frac{1}{2})) - \Phi'(\lambda, \gamma(b - \frac{1}{2})) \right) - \int_{-\infty}^{\infty} d\mu K_1(\lambda - \mu) \rho^{(2)}(\mu), \\ \rho^{(2)}(\lambda) &= \frac{1}{4\pi} \left( \Phi'(\lambda, \gamma(b + \frac{1}{2})) - \Phi'(\lambda, \gamma(b - \frac{1}{2})) \right) - \int_{-\infty}^{\infty} d\mu K_1(\lambda - \mu) \rho^{(1)}(\mu), \end{aligned} \quad (4.7)$$

with

$$K_1(\lambda) = \frac{1}{2\pi} \Phi'(\lambda, \gamma) = \frac{1}{\pi} \frac{\sin(2\gamma)}{\cosh 2\lambda - \cos 2\gamma}. \quad (4.8)$$

Eqs. (4.7) can be solved by Fourier transformation giving

$$\rho^{(1)}(\lambda) = \rho^{(2)}(\lambda) = \frac{1}{\gamma} \frac{\cos(\pi b) \cosh\left(\frac{\pi\lambda}{\gamma}\right)}{\cosh\left(\frac{2\pi\lambda}{\gamma}\right) + \cos(2\pi b)}. \quad (4.9)$$

Using this expression we can compute the energy density  $e_\infty^{(A1)} = E/L$  of the antiferromagnetic ground state from the infinite volume limit of Eq. (2.12):

$$e_\infty^{(A1)} = -4 \int_{-\infty}^{\infty} d\omega \frac{\cosh^2(b\gamma\omega) \sinh((\pi - \gamma)\omega/2)}{\sinh(\pi\omega/2) \cosh(\gamma\omega/2)} \quad \text{for } 0 \leq \gamma < \pi/2 \quad \text{and } 0 \leq b < \frac{1}{2}. \quad (4.10)$$

Low-lying excitations over this ground state are described by modifications of the configuration of Bethe roots, e.g. by alternative choices for the integers  $Q_j^{(a)}$ . The excitations have a linear dispersion which is found to be  $\epsilon^{(a)}(\lambda) \sim v_{A1}^{(mix)} p^{(a)}(\lambda)$  by standard methods [31]. In the present model we obtain

$$v_{A1}^{(mix)} = \frac{1}{4\pi\rho^{(a)}(\lambda)} \left. \frac{\partial \epsilon^{(a)}(\lambda)}{\partial \lambda} \right|_{\lambda=\infty} = \frac{\pi}{\gamma}, \quad (4.11)$$

independent of the representation parameter  $b$ .

#### *Analysis of the finite-size spectrum – anti-ferromagnetic regime*

Refining the root density approach used above to compute the thermodynamic properties of the antiferromagnetic ground state the finite-size corrections to the low-lying energy levels can be computed [31–35]. In agreement with the predictions [36, 37] of conformal field theory they are found to be of the form

$$E(L, \gamma) - L e_\infty^{(A1)} = \frac{2\pi v_{A1}}{L} \left[ -\frac{1}{6} + X_{n_1, n_2}^{m_1, m_2}(\gamma) \right] + o(L^{-1}), \quad (4.12)$$

where the scaling dimensions  $X_{n_1, n_2}^{m_1, m_2}(\gamma)$  are given by

$$\begin{aligned} X_{n_1, n_2}^{m_1, m_2}(\gamma) = & \frac{\pi - \gamma}{4\pi} (n_1 + n_2)^2 + \frac{\pi}{4(\pi - \gamma)} (m_1 + m_2)^2 \\ & + \frac{\gamma}{4\pi} (n_1 - n_2)^2 + \frac{\pi}{4\gamma} (m_1 - m_2)^2. \end{aligned} \quad (4.13)$$

Here the integers  $n_a$ ,  $a = 1, 2$ , are related to the numbers of Bethe roots on each level by  $N_a = L - n_a$  and therefore determine the conserved  $U(1)$  charge and spin of the excitation to be  $B = (n_1 - n_2)/2$



and  $S_3 = (n_1 + n_2)/2$ . The macroscopic momentum (vorticity) of the excitations is determined by the indices  $m_a$ . As a consequence of the selection rule (4.4) they take integer (half-odd integer) values depending on the parity of  $n_1 \pm n_2$ :

$$\begin{aligned} \bullet \quad & \text{for } n_1 \pm n_2 \text{ odd} & \rightarrow & m_1, m_2 = 0, \pm 1, \pm 2, \dots \\ \bullet \quad & \text{for } n_1 \pm n_2 \text{ even} & \rightarrow & m_1, m_2 = \pm \frac{1}{2}, \pm \frac{3}{2}, \pm \frac{5}{2}, \dots \end{aligned} \quad (4.14)$$

Note that the scaling dimensions (4.13) always decompose into two parts depending on the charge and spin quantum numbers of the excitation separately. In the continuum theory the excitations are free bosons with compactification radii  $R_c^2 = 2\gamma/\pi = 2 - R_s^2$ , respectively.

### Numerical results

To verify our expression (4.13) for the scaling dimensions with the selection rule (4.14) we have identified some of the corresponding configurations of Bethe roots and solved the Bethe equations (2.10) numerically for lattice sizes up to  $L = 100$ . From the numerical data for the energy eigenvalues (2.12) we then compute the sequence

$$X(L, \gamma) = \frac{L}{2\pi v_{A1}} \left( E(L, \gamma) - L e_\infty^{(A1)} \right) + \frac{1}{6} \quad (4.15)$$

which in the thermodynamic limit is expected to extrapolate to the dimensions (4.13). In Table I we present the finite-size estimates for the energy of the antiferromagnetic ground state  $E_0(L)$  for  $\gamma = 2\pi/5$  and  $2\pi/9$  and  $b = 0.1, 0.2, 0.3, 0.4$ . Extrapolation of the data gives the predicted value  $X_{1,0}^{0,0} = 1/4$ , independent of the deformation parameter  $\gamma$  and the representation parameter  $b$ . The corresponding finite-size scaling of the ground state energy is

$$E_0(L, \gamma) - L e_\infty^{(A1)} = \frac{2\pi v_{A1}}{L} \frac{1}{12} + o(L^{-1}) = \frac{\pi v_{A1}}{6L} + o(L^{-1}) \quad (4.16)$$

corresponding to a central charge  $c = -1$  of the continuum theory. This coincides with the result from [16] for the  $U_q[osp(2|2)]$  chain at  $b = 0$ .

Further support for the proposed critical theory is given by corresponding analysis of the finite-size behaviour of excitation energies:

- a state corresponding to the  $X_{0,0}^{\frac{1}{2}, \frac{1}{2}} = \frac{1}{4} (1 - \gamma/\pi)^{-1}$  is described by  $(N_1, N_2) = (L, L - 1)$  real Bethe roots distributed symmetrically around the origin plus a single root  $\lambda^{(2)} = i\pi/2$  on the second level. The finite-size data and their extrapolation for this state are presented in Table II.

- the dimension  $X_{1,-1}^{\frac{1}{2},\frac{1}{2}} = (\gamma/\pi) + \frac{1}{4}(1 - \gamma/\pi)^{-1}$  is found in the sector  $(N_1, N_2) = (L+1, L-1)$  and given by  $(L, L-1)$  real roots distributed symmetrically around the origin plus a single root  $\lambda^{(1)} = i\pi/2$  on the first level. The numerical data are given in Table III.
- the configuration of Bethe roots for the state corresponding to  $X_{1,0}^{1,0} = \frac{1}{4} + (\pi/4\gamma) + \frac{1}{4}(1 - \gamma/\pi)^{-1}$  consists of  $(L-1, L-1)$  real rapidities and a single additional root on the line  $\text{Im}(\lambda^{(a)}) = \pi/2$  in one level. Numerical results are found in Table IV.
- The configuration of roots for  $X_{1,1}^{\frac{1}{2},\frac{1}{2}} = 1 + (\gamma/\pi) + \frac{1}{4}(1 - \gamma/\pi)^{-1}$  has two special features: considering the  $(L, L-1)$  sector we find that there is one root  $\lambda^{(2)}$  which is situated at  $\infty$ . Within the root density formalism this leads to a phase shift of  $\gamma$  in the logarithmic equations (4.2) for the remaining  $(L, L-2)$  roots (see [17]). The configuration of these roots changes at  $\gamma = \pi/3$  from all real to  $(L-1, L-2)$  real and one first level root with imaginary part  $\pi/2$  (such a situation has also been found in the Bethe ansatz solution of the twisted XXZ chain [38]). The finite-size data for (4.15) are shown in Table V.
- Finally, the state with  $X_{1,0}^{1,1} = \frac{1}{4} + (1 - \gamma/\pi)^{-1}$  in the zero charge sector  $(L-1, L-1)$  is given by a solution of the Bethe equations (3.9) corresponding to the degenerated XXZ sector of the mixed superspin chain. The finite-size estimates and the extrapolation for the dimension are given in Table VI.

Summarizing the results of this section we have found that the critical behaviour of the anti-ferromagnetic mixed superspin chain does not depend on the staggering as long as  $|b| < \frac{1}{2}$ . It is described by a  $c = -1$  conformal field theory identical to the one obtained before in the context of the antiferromagnetic  $U_q[\text{osp}(2|2)]$  chain, i.e. for  $b = 0$  [16].

### B. Phase A2: ferromagnetic regime for $0 \leq b \leq 1/2$

Let us now turn to the ferromagnetic regime of the mixed superspin chain. As discussed above, we can use the spectral relation  $\text{spec}(H^{(mix)}(\gamma)) = \text{spec}(-H^{(mix)}(\pi - \gamma))$  to discuss this regime in the interval of anisotropies  $0 \leq \gamma \leq \pi/2$  using the opposite sign for the energy eigenvalues (2.12). As a consequence, the classification of solutions to the Bethe equations (2.10) remains unchanged.

*Thermodynamic limit*

From exact diagonalization of the Hamiltonian for small system sizes we find that the low energy states can be identified with configurations where the Bethe roots with  $\text{Im}(\lambda_j^{(a)}) = \pi/2$ . As in the antiferromagnetic case the ground state in this regime is four-fold degenerate and has charge  $B = \pm \frac{1}{2}$  and spin  $S_3 = \pm \frac{1}{2}$  corresponding to the sectors  $(N_1, N_2) = (L, L-1)$  and  $(L-1, L)$  of the Bethe equations. Reparameterisation of the rapidities as  $\lambda_j^{(a)} = \mu_j^{(a)} + i\pi/2$  and taking the logarithm of (2.10) we obtain

$$\begin{aligned} L \left[ \Psi(\mu_j^{(1)}, \gamma(b+1/2)) - \Psi(\mu_j^{(1)}, \gamma(b-1/2)) \right] &= 2\pi R_j^{(1)} - \sum_{k=1}^{N_2} \Phi(\mu_j^{(1)} - \mu_k^{(2)}, \gamma), \quad j = 1, \dots, N_1 \\ L \left[ \Psi(\mu_j^{(2)}, \gamma(b+1/2)) - \Psi(\mu_j^{(2)}, \gamma(b-1/2)) \right] &= 2\pi R_j^{(2)} - \sum_{k=1}^{N_1} \Phi(\mu_j^{(2)} - \mu_k^{(1)}, \gamma), \quad j = 1, \dots, N_2 \end{aligned} \quad (4.17)$$

where

$$\Psi(x, y) = 2 \arctan(\tanh(x) \tan(y)) \quad (4.18)$$

and  $\Phi(x, y)$  has been defined in Eq. (4.3). Again, the numbers  $R_j^{(a)}$  define the branches of the logarithm and have to be chosen integer or half-odd integer depending on the parities of  $N_a$  according to the rule

$$R_j^{(1)} \equiv \frac{N_2}{2} \pmod{1}, \quad R_j^{(2)} \equiv \frac{N_1}{2} \pmod{1}. \quad (4.19)$$

To analyze the thermodynamic limit in this parameter region we proceed as above: for  $L \rightarrow \infty$  the roots  $\mu_j^{(a)}$  fill the real axis with densities

$$\sigma^{(a)}(\mu) = \frac{1}{(\pi - \gamma)} \frac{\cos \left[ \frac{\pi b \gamma}{\pi - \gamma} \right] \cosh \left[ \frac{\pi \mu}{\pi - \gamma} \right]}{\cosh \left[ \frac{2\pi \mu}{\pi - \gamma} \right] + \cos \left[ \frac{2\pi b \gamma}{\pi - \gamma} \right]}, \quad \text{for } a = 1, 2. \quad (4.20)$$

As before we can now compute the energy density of the ferromagnetic ground state from (2.12) with the result

$$e_\infty^{(A2)} = -4 \int_{-\infty}^{\infty} d\omega \frac{\cosh[\omega b \gamma]^2 \sinh[\omega \gamma/2]}{\sinh[\omega \pi/2] \cosh[\omega(\pi - \gamma)/2]} \quad \text{for } 0 < \gamma \leq \pi/2 \text{ and } 0 \leq b \leq 1/2. \quad (4.21)$$

The low-lying excitations have a linear dispersion  $\epsilon^{(a)}(\mu) \sim v_{A2}^{(mix)} p^{(a)}(\mu)$  with Fermi velocity

$$v_{A2}^{(mix)} = \left. \frac{\partial_\mu \epsilon^{(a)}(\mu)}{4\pi \sigma^{(a)}(\mu)} \right|_{\mu=\infty} = \frac{\pi}{\pi - \gamma}. \quad (4.22)$$

*Analysis of the finite-size spectrum – ferromagnetic regime*

The computation of finite-size corrections to the low-lying energy levels over the ferromagnetic ground state within the root density formalism is completely analogous to the antiferromagnetic regime above. We find that the scaling dimensions are

$$\begin{aligned} X_{n_1, n_2}^{m_1, m_2}(\gamma) = & \frac{\pi - \gamma}{4\pi} (n_1 - n_2)^2 + \frac{\pi}{4(\pi - \gamma)} (m_1 - m_2)^2 \\ & + \frac{\gamma}{4\pi} (n_1 + n_2)^2 + \frac{\pi}{4\gamma} (m_1 + m_2)^2. \end{aligned} \quad (4.23)$$

Again the integers  $n_a$ ,  $a = 1, 2$ , determine the conserved  $U(1)$  charge and spin of the corresponding excitation while the vorticity of the state is given by the  $m_a$ . The latter are integer (half-odd integer) depending on the parity of  $n_1 \pm n_2$ :

$$\begin{aligned} \bullet \quad \text{for } n_1 \pm n_2 \text{ odd} & \quad \rightarrow \quad m_1, m_2 = 0, \pm 1, \pm 2, \dots \\ \bullet \quad \text{for } n_1 \pm n_2 \text{ even} & \quad \rightarrow \quad m_1, m_2 = \pm \frac{1}{2}, \pm \frac{3}{2}, \pm \frac{5}{2}, \dots \end{aligned} \quad (4.24)$$

As in the low-energy spectrum of the antiferromagnetic mixed superspin chain we find an exact separation of spin and charge degrees of freedom. The compactification radii, however, are interchanged.

*Numerical results*

To support these results for the scaling dimensions (4.23) with (4.24) we have identified the Bethe configurations corresponding to several states and studied the  $L$ -dependence of the corresponding energies using the estimators

$$X(L) = \frac{L}{2\pi v_{A2}} \left( E(L, \gamma) - L e_{\infty}^{(A2)} \right) + \frac{1}{6} \quad (4.25)$$

which in the thermodynamic limit is expected to extrapolate to the dimensions (4.23):

- the ferromagnetic ground state is described by  $(N_1, N_2) = (L, L - 1)$  roots on the line  $\text{Im}(\lambda_j^{(a)}) = \pi/2$ , with density approaching Eq. (4.20) in the thermodynamic limit. The finite-size data (4.25) extrapolate to  $X_{0,1}^{0,0}(\gamma) = X_{1,0}^{0,0}(\gamma) \equiv 1/4$  independently of  $\gamma$  and the representation parameter  $b$  (see Table VII). As a consequence the ground state energy scales like

$$E_0(L, \gamma) - L e_{\infty}^{(A2)} = \frac{\pi v_{A2}}{6L} + o(L^{-1}) \quad (4.26)$$

corresponding to a low energy effective theory with central charge  $c = -1$ .

- the state giving the scaling dimension  $X_{0,0}^{\frac{1}{2},-\frac{1}{2}} = \frac{1}{4}(1 - \gamma/\pi)^{-1}$  is found in the sector with  $L$  roots with  $\text{Im}(\lambda_j^{(a)}) = \pi/2$  for each level. Two configuration of this type exist which are mapped onto each other by reflection at the imaginary axis. They have one root on each level at  $\lambda^{(1)} = -\lambda^{(2)} = \pm\infty$ . The numerical data for the scaling dimensions are shown in Table VIII.
- a similar configuration in the sector  $(L-1, L-1)$  and without the roots at  $\pm\infty$  gives rise to the dimension  $X_{1,1}^{\frac{1}{2},-\frac{1}{2}} = (\gamma/\pi) + \frac{1}{4}(1 - \gamma/\pi)^{-1}$ , see Table IX.
- the scaling dimension  $X_{1,1}^{\frac{1}{2},\frac{1}{2}} = (\gamma/\pi) + (\pi/4\gamma)$  is in the degenerated XXZ sector of the mixed superspin chain and corresponds to a solution of (3.9) with  $N = L-1$ . For  $\gamma > \pi/4$  all of the roots have imaginary part  $\pi/2$ , at  $\gamma = \pi/4$  the first of these roots jumps to the real axis. The finite size extrapolation of  $X_{1,1}^{\frac{1}{2},\frac{1}{2}}$  is shown in Table X.
- the configuration of Bethe roots corresponding to  $X_{1,0}^{1,-1} = \frac{1}{4} + (1 - \gamma/\pi)^{-1}$  is in the  $(L, L-1)$  sector with  $(L-1, L-1)$  roots on the line  $\text{Im}(\lambda^{(a)}) = \pi/2$  where one of the roots on the second level is at  $\infty$ . In addition there exists a single real root  $\lambda^{(1)}$ . The finite-size data are in Table XI.
- The state leading to  $X_{0,0}^{\frac{1}{2},\frac{1}{2}} = (\pi/4\gamma)$  is again in the degenerate XXZ sector determined by the equations (3.9). It consists of  $L-1$  roots with imaginary part  $\pi/2$  and a single real root for  $\gamma > \pi/4$ . Below  $\gamma = \pi/4$  the configuration changes into  $L-2$  roots  $\text{Im}(\lambda) = \pi/2$  and a pair of complex conjugate roots forming a 2-string. Lowering  $\gamma$  further it is expected that longer strings are formed, similar as observed in [17]. The energy of the state depends on  $\gamma$  in a continuous way, the extrapolation of the finite-size data can be found in Table XII.

As in the antiferromagnetic regime the scaling dimensions obtained both from our analysis of the thermodynamic limit and by solving the Bethe equations for the mixed superspin chain in this phase do not depend on the staggering  $b$ . In fact, the scaling dimensions (4.23) coincide with what has been found previously for the mixed superspin chain constructed from alternating three-dimensional quark and antiquark representations of  $U_q[sl(2|1)]$  which is related to the present model in the limit  $b \rightarrow \frac{1}{2}$  [17]: we conclude that the critical theory of the mixed model is the same as that for the critical  $U_q[osp(2|2)]$  spin chain for *all*  $|b| \leq \frac{1}{2}$  and has an effective central charge  $c = -1$ .

## V. THE *FERROMAGNETIC* MIXED SUPERSPIN CHAIN FOR $b > \frac{1}{2}$

Numerically diagonalizing the Hamiltonian (2.11) for parameters  $0 < \gamma < \pi/2$  and  $\frac{1}{2} < b \leq \pi/4\gamma$  we find the ground state of the ferromagnetic model, i.e. with Hamiltonian  $-\mathcal{H}^{(mix)}$ , in the sectors  $(N_1, N_2) = (L \pm 1, L \mp 1)$ , i.e. two degenerate singlets with charge  $B = \pm 1$  and spin  $S_3 = 0$ , respectively. For the self-dual model,  $\gamma b = \pi/4$ , the degeneracy of this ground state is doubled for even  $L$  as a consequence of the additional discrete  $\mathbb{Z}_2$  symmetry on this line. For the low energy states we have identified the corresponding root configurations solving the Bethe equations (2.10): they are organized into strings (4.1) of length 1 with both parities, i.e.  $(1, \pm)$ -strings. Hence we consider solutions

$$\left\{ \lambda_j^{(a)} \right\}_{j=1}^{N_a} \equiv \left\{ \lambda_j^{(a)} \right\}_{j=1}^{N_a^+} \cup \left\{ \mu_j^{(a)} + i\frac{\pi}{2} \right\}_{j=1}^{N_a^-}, \quad a = 1, 2 \quad (5.1)$$

of the Bethe equations with  $N_a = N_a^+ + N_a^-$  real parameters  $\lambda_j^{(a)}$  and  $\mu_j^{(a)}$ . Taking the logarithm of (2.10) we obtain

$$\begin{aligned} L \left( \Phi(\lambda_j^{(1)}, \gamma(b + \frac{1}{2})) - \Phi(\lambda_j^{(1)}, \gamma(b - \frac{1}{2})) \right) &= 2\pi Q_j^{(1)} \\ &+ \sum_{k=1}^{N_2^+} \Phi(\lambda_j^{(1)} - \lambda_k^{(2)}, \gamma) - \sum_{k=1}^{N_2^-} \Psi(\lambda_j^{(1)} - \mu_k^{(2)}, \gamma), \quad j = 1, \dots, N_1^+, \\ -L \left( \Psi(\mu_j^{(1)}, \gamma(b + \frac{1}{2})) - \Psi(\mu_j^{(1)}, \gamma(b - \frac{1}{2})) \right) &= 2\pi R_j^{(1)} \\ &- \sum_{k=1}^{N_2^+} \Psi(\mu_j^{(1)} - \lambda_k^{(2)}, \gamma) + \sum_{k=1}^{N_2^-} \Phi(\mu_j^{(1)} - \mu_k^{(2)}, \gamma), \quad j = 1, \dots, N_1^-, \\ L \left( \Phi(\lambda_j^{(2)}, \gamma(b + \frac{1}{2})) - \Phi(\lambda_j^{(2)}, \gamma(b - \frac{1}{2})) \right) &= 2\pi Q_j^{(2)} \\ &+ \sum_{k=1}^{N_1^+} \Phi(\lambda_j^{(2)} - \lambda_k^{(1)}, \gamma) - \sum_{k=1}^{N_1^-} \Psi(\lambda_j^{(2)} - \mu_k^{(1)}, \gamma), \quad j = 1, \dots, N_2^+, \\ -L \left( \Psi(\mu_j^{(2)}, \gamma(b + \frac{1}{2})) - \Psi(\mu_j^{(2)}, \gamma(b - \frac{1}{2})) \right) &= 2\pi R_j^{(2)} \\ &- \sum_{k=1}^{N_1^+} \Psi(\mu_j^{(2)} - \lambda_k^{(1)}, \gamma) + \sum_{k=1}^{N_1^-} \Phi(\mu_j^{(2)} - \mu_k^{(1)}, \gamma), \quad j = 1, \dots, N_2^-, \end{aligned} \quad (5.2)$$

where  $\Phi(x, y)$  and  $\Psi(x, y)$  have been introduced in Eqs. (4.3) and (4.18) above. The quantum numbers  $Q_j^{(a)}$ ,  $R_j^{(a)}$  arise from specifying the branch of the logarithm and uniquely characterize an eigenstate of the system. They have to be chosen integer or half-odd integer according to the

parities of the numbers  $N_a^\pm$ :

$$\begin{aligned} Q_j^{(1)} &\equiv \frac{N_2^+}{2} \pmod{1}, & R_j^{(1)} &\equiv \frac{N_2^-}{2} \pmod{1}, \\ Q_j^{(2)} &\equiv \frac{N_1^+}{2} \pmod{1}, & R_j^{(2)} &\equiv \frac{N_1^-}{2} \pmod{1}. \end{aligned} \quad (5.3)$$

### A. Thermodynamic limit

We introduce counting functions for the relevant root configurations (5.1)

$$\begin{aligned} z^{(1)}(\lambda) &= \frac{1}{2} \left( \Phi(\lambda, \gamma(b + \frac{1}{2})) - \Phi(\lambda, \gamma(b - \frac{1}{2})) \right) - \frac{1}{2L} \sum_{k=1}^{N_2^+} \Phi(\lambda - \lambda_k^{(2)}, \gamma) + \frac{1}{2L} \sum_{k=1}^{N_2^-} \Psi(\lambda - \mu_k^{(2)}, \gamma), \\ y^{(1)}(\mu) &= -\frac{1}{2} \left( \Psi(\mu, \gamma(b + \frac{1}{2})) - \Psi(\mu, \gamma(b - \frac{1}{2})) \right) + \frac{1}{2L} \sum_{k=1}^{N_2^+} \Psi(\mu - \lambda_k^{(2)}, \gamma) - \frac{1}{2L} \sum_{k=1}^{N_2^-} \Phi(\mu - \mu_k^{(2)}, \gamma), \end{aligned} \quad (5.4)$$

and, similarly,  $z^{(2)}(\lambda)$ ,  $y^{(2)}(\mu)$ . Evaluating the counting functions at a root of Eq. (5.2) yields the corresponding quantum number up to a factor of  $\pi/L$ , e.g.  $z^{(a)}(\lambda_j^{(a)}) = \pi Q_j^{(a)}/L$ . Taking the thermodynamic limit  $L \rightarrow \infty$  with fixed ratios  $N_a^\pm/L$  the derivatives of the counting functions define the densities of roots  $\rho^{(a)}$ ,  $\sigma^{(a)}$  and 'holes'  $\rho_h^{(a)}$ ,  $\sigma_h^{(a)}$ .

$$\begin{aligned} 2\pi \left( \rho^{(a)}(\lambda) + \rho_h^{(a)}(\lambda) \right) &= -\frac{dz^{(a)}(\lambda)}{d\lambda}, \\ 2\pi \left( \sigma^{(a)}(\mu) + \sigma_h^{(a)}(\mu) \right) &= -\frac{dy^{(a)}(\mu)}{d\mu}. \end{aligned} \quad (5.5)$$

The signs are chosen such that the bare densities, i.e. the hole densities in the reference state  $N_a^\pm = 0$

$$\begin{aligned} \rho_0(\lambda) &= -\frac{1}{4\pi} \left( \Phi'(\lambda, \gamma(b + \frac{1}{2})) - \Phi'(\lambda, \gamma(b - \frac{1}{2})) \right) \\ &= -\frac{1}{2\pi} \left( \frac{\sin 2\gamma(b + \frac{1}{2})}{\cosh 2\lambda - \cos 2\gamma(b + \frac{1}{2})} - \frac{\sin 2\gamma(b - \frac{1}{2})}{\cosh 2\lambda - \cos 2\gamma(b - \frac{1}{2})} \right), \\ \sigma_0(\lambda) &= \frac{1}{4\pi} \left( \Psi'(\lambda, \gamma(b + \frac{1}{2})) - \Psi'(\lambda, \gamma(b - \frac{1}{2})) \right) \\ &= \frac{1}{2\pi} \left( \frac{\sin 2\gamma(b + \frac{1}{2})}{\cosh 2\lambda + \cos 2\gamma(b + \frac{1}{2})} - \frac{\sin 2\gamma(b - \frac{1}{2})}{\cosh 2\lambda + \cos 2\gamma(b - \frac{1}{2})} \right), \end{aligned} \quad (5.6)$$

are positive near the origin. Note, however, that  $\rho_0(\lambda)$  changes sign at  $\cosh(2\lambda_0) = \cos \gamma / \cos(2\gamma b)$ . On the line  $\gamma b = \pi/4$ , where the model is self-dual under the transformation (2.13),  $\lambda_0 = \pm\infty$  such that  $\rho_0(\lambda)$  is non-negative for real  $\lambda$ . Away from this line, however,  $\lambda_0$  is finite which will require special attention in the analysis of the thermodynamic limit within the root density formalism

below. For now, we proceed as in the previous sections and arrive at integral equations for the densities

$$\begin{pmatrix} \rho^{(1)}(\lambda) \\ \sigma^{(1)}(\lambda) \\ \rho^{(2)}(\lambda) \\ \sigma^{(2)}(\lambda) \end{pmatrix} = \begin{pmatrix} \rho_0(\lambda) \\ \sigma_0(\lambda) \\ \rho_0(\lambda) \\ \sigma_0(\lambda) \end{pmatrix} + \int_{-\infty}^{\infty} d\mu \mathbb{K}(\lambda - \mu) \begin{pmatrix} \rho^{(1)}(\mu) \\ \sigma^{(1)}(\mu) \\ \rho^{(2)}(\mu) \\ \sigma^{(2)}(\mu) \end{pmatrix} \quad (5.7)$$

with kernel matrix

$$\mathbb{K}(\lambda) = \begin{pmatrix} 0 & 0 & K_1(\lambda) & -K_2(\lambda) \\ 0 & 0 & -K_2(\lambda) & K_1(\lambda) \\ K_1(\lambda) & -K_2(\lambda) & 0 & 0 \\ -K_2(\lambda) & K_1(\lambda) & 0 & 0 \end{pmatrix}. \quad (5.8)$$

The function  $K_1(\lambda)$  has been given before in (4.8) and

$$K_2(\lambda) = \frac{1}{2\pi} \Psi'(\lambda, \gamma) = \frac{1}{\pi} \frac{\sin(2\gamma)}{\cosh 2\lambda + \cos 2\gamma}. \quad (5.9)$$

Solving the integral equations (5.7) by Fourier transformation one obtains

$$\begin{aligned} \rho^{(a)}(\lambda) &= \frac{\sin \frac{\pi\gamma(2b-1)}{\pi-2\gamma}}{2(\pi-2\gamma)} \left( \cosh \frac{2\pi\lambda}{\pi-2\gamma} - \cos \frac{\pi\gamma(2b-1)}{\pi-2\gamma} \right)^{-1}, \\ \sigma^{(a)}(\lambda) &= \frac{\sin \frac{\pi\gamma(2b-1)}{\pi-2\gamma}}{2(\pi-2\gamma)} \left( \cosh \frac{2\pi\lambda}{\pi-2\gamma} + \cos \frac{\pi\gamma(2b-1)}{\pi-2\gamma} \right)^{-1}, \end{aligned} \quad (5.10)$$

for  $a = 1, 2$ , corresponding to total densities

$$\frac{N_a^+}{2L} = \int_{-\infty}^{\infty} d\lambda \rho^{(a)}(\lambda) = \frac{1}{2} \frac{\pi - 2\gamma b - \gamma}{\pi - 2\gamma} = \frac{1}{2} - \frac{N_a^-}{2L}. \quad (5.11)$$

On the self-dual line  $\gamma b = \pi/4$  the densities  $\rho^{(a)}$  and  $\sigma^{(a)}$  coincide. In the limit  $b \rightarrow \frac{1}{2}$  the densities of  $(1, -)$ -strings vanish, indicating the transition to the ground state of phase A2 (see also Ref. 17).

Note that the densities (5.10) are positive for real  $\lambda$  in the entire phase B, hence a consistent description of the thermodynamic limit of this state within the root density formalism is possible. Using (5.10) in (2.12) we obtain the energy density of this eigenstate of the ferromagnetic superspin chain:

$$\begin{aligned} \epsilon_{\infty}^{(B)} &\equiv \lim_{L \rightarrow \infty} \frac{1}{L} E_{N_1^{\pm}, N_2^{\pm}}^{(mix)} = -4\pi \sum_{a=1,2} \left[ \int_{-\infty}^{\infty} d\lambda \rho_0(\lambda) \rho^{(a)}(\lambda) + \int_{-\infty}^{\infty} d\mu \sigma_0(\mu) \sigma^{(a)}(\mu) \right] \\ &= -4 \int_{-\infty}^{\infty} d\omega \frac{\sinh(\gamma\omega/2) (\sinh((\pi - \gamma)\omega/2) \cosh((\pi/2 - 2\gamma b)\omega) - \sinh(\gamma\omega/2))}{\sinh(\pi\omega/2) \sinh((\pi - 2\gamma)\omega/2)}. \end{aligned} \quad (5.12)$$

Starting from this state we find that there are low energy excitations with linear dispersion. Their Fermi velocity is

$$v_B = \frac{2\pi}{\pi - 2\gamma}. \quad (5.13)$$



### B. Phase B: critical theory of the self-dual model

As noted above the description of the thermodynamic limit above is guaranteed to yield the ground state for parameters satisfying the self-duality condition  $\gamma b = \pi/4$ . Therefore we begin our discussion of the low energy behaviour for this case.

#### *Finite-size spectrum*

The finite-size corrections for the low energy spectrum of the superspin chain on the self-dual line can again be studied based on the root density approach. Unlike in the cases discussed in the previous sections, however, particular combinations of quantum numbers for the vorticities of the four low energy modes lead to a singular contribution to the finite-size energy. This can be traced back to a singularity of the integral kernel in (5.7), i.e. the fact that one of the eigenvalues of  $(1 - \tilde{\mathbb{K}}(\omega = 0))$  vanishes. This situation is similar to that found previously for the mixed superspin chain based on the atypical  $b = \pm \frac{1}{2}$  representations of  $U_q[sl(2|1)]$  [5, 17] as well as for the ferromagnetic staggered six-vertex model (3.1) with  $\gamma b = \pi/4$  [6, 39]. As advocated in the aforementioned works this subtlety can be taken care of by proper regularization the integral operator and leads to strong logarithmic finite-size corrections for the contributions from the singular mode. Put into the present context these considerations leads us to the following proposal for the general form of the low energy spectrum

$$E(L, \gamma) - L\varepsilon_\infty^{(B)}(\gamma) = \frac{2\pi v_B}{L} \left[ -\frac{1}{3} + X_{n_1^+, n_1^-, n_2^+, n_2^-}^{m_1^+, m_1^-, m_2^+, m_2^-}(\gamma) \right] + o(L^{-1}). \quad (5.14)$$

The scaling dimensions depend on the quantum numbers of the four massless modes with Fermi velocities (5.13) in this phase:

$$\begin{aligned} X_{n_1^+, n_1^-, n_2^+, n_2^-}^{m_1^+, m_1^-, m_2^+, m_2^-}(\gamma) &= \frac{\gamma}{4\pi} (n_1^+ + n_1^- + n_2^+ + n_2^-)^2 + \frac{\pi}{16\gamma} (m_1^+ + m_1^- + m_2^+ + m_2^-)^2 \\ &+ \frac{\pi - 2\gamma}{8\pi} (n_1^+ + n_1^- - n_2^+ - n_2^-)^2 + \frac{\pi}{8(\pi - 2\gamma)} (m_1^+ + m_1^- - m_2^+ - m_2^-)^2 \\ &+ \frac{1}{8} (n_1^+ - n_1^- - n_2^+ + n_2^-)^2 + \frac{1}{8} (m_1^+ - m_1^- - m_2^+ + m_2^-)^2 \\ &+ \frac{K(L)}{8} (n_1^+ - n_1^- + n_2^+ - n_2^-)^2 + \frac{1}{8K(L)} (m_1^+ - m_1^- + m_2^+ - m_2^-)^2. \end{aligned} \quad (5.15)$$

The excitations are labeled by  $n_a^\pm = (L/2) - N_a^\pm$ , i.e. the difference between the number of Bethe roots in (5.1) and the ground state densities (5.11) on the line  $b\gamma = \pi/4$  in the thermodynamic limit. By definition the  $n_a^\pm$  are integers (half-odd integers) for lattices with even (odd)  $L$ . From the

selection rule (5.3) we conclude that the vorticities of an excitation with charges  $(n_1^+, n_1^-, n_2^+, n_2^-)$  are integer or half-odd integer values according to the rule

$$m_a^\pm = \frac{1}{2} (n_1^\pm - n_2^\pm + 1) \mod 1, \quad a = 1, 2. \quad (5.16)$$

The difference  $n_1^\pm - n_2^\pm \equiv -(N_1^\pm - N_2^\pm)$  is always integer, therefore the vorticities can take integer or half-odd integer values depending on the numbers  $n_a^\pm$ .

Two of the gapless modes contributing to (5.15) can be identified with the  $U(1)$  symmetries corresponding to spin and charge of the mixed superspin chain: the effective theories for these modes are those of free bosons with compactification radii  $R_s^2 = 4\gamma/\pi = 2 - R_c^2$ . The existence of the third compact boson with radius  $(R_3)^2 = 2$  does not follow directly from the symmetries of the mixed superspin chain.

The coupling constant  $K(L)$  of the fourth mode reflects the effect of the regularization of the integral operator on the finite lattice: an analytical derivation of its  $L$ -dependence does not exist so far. Based on numerical evidence  $K(L)$  is expected to display a logarithmic dependence on the lattice size  $L$  and to vanish as  $L \rightarrow \infty$ . Later on we shall present our own numerical results supporting such finite-size logarithmic corrections for the superspin chain. Here we draw on previous studies of the staggered ferromagnetic six-vertex model [6]: as discussed in Section III the scaling dimensions (5.15) with  $n_1^\pm = n_2^\pm = n^\pm$ ,  $m_1^\pm = m_2^\pm = m^\pm$  appear in the XXZ subsector of the spectrum. Taking into account (3.10) the finite-size spectrum of the staggered XXZ model is

$$\begin{aligned} E^{(6v)}(L, \gamma) - \frac{L}{2} \varepsilon_\infty^{(B)}(\gamma) &= \frac{2\pi v_B}{L} \left[ -\frac{1}{6} + \tilde{X}_{n^+, n^-}^{m^+, m^-}(\gamma) \right] + o(L^{-1}), \\ \tilde{X}_{n^+, n^-}^{m^+, m^-}(\gamma) &= \frac{\gamma}{2\pi} (n^+ + n^-)^2 + \frac{\pi}{8\gamma} (m^+ + m^-)^2 \\ &\quad + \frac{K(L)}{4} (n^+ - n^-)^2 + \frac{1}{4K(L)} (m^+ - m^-)^2. \end{aligned} \quad (5.17)$$

Note that both the charge mode *and* the boson with self-dual radius  $R_3^2 = 2$  disappear from the spectrum in this sector. The scaling dimensions  $\tilde{X}_{n^+, n^-}^{m^+, m^-}(\gamma)$  have been obtained directly for the staggered six vertex model previously [39].

Finally let us remark on the effect of boundary conditions on the finite-size spectrum: for antiperiodic boundary conditions, i.e. twist  $\varphi = \pi$  in (3.4), relevant for the staggered six vertex model hidden inside the superspin chain the vorticities are constrained by  $m^\pm = \varphi/2\pi \mod 1$ , hence they take half odd integer values.

### Numerical results

As mentioned at the beginning of this section one of the ground states of the mixed superspin chain is in the sector  $(N_1, N_2) = (L+1, L-1)$  corresponding to charge  $B = +1$  and zero magnetization. Following the selection rules for the  $n_a^\pm, m_a^\pm$  given above we find the lowest energy state for odd  $L$  in this sector to be given by  $\mathbf{n} \equiv (n_1^+, n_1^-, n_2^+, n_2^-) = (-\frac{1}{2}, -\frac{1}{2}, \frac{1}{2}, \frac{1}{2})$  and  $\mathbf{m} = (0, 0, 0, 0)$ . According to (5.14) the ground state energy scales as

$$E_0(L, \gamma) - L\varepsilon_\infty^{(B)}(\gamma) = -\frac{\pi v_B}{6L} \left[ 2\frac{6\gamma - \pi}{\pi} \right] + o(L^{-1}), \quad (5.18)$$

giving an effective central charge  $c_{\text{eff}} = 2(6\gamma - \pi)/\pi$ . Note that  $c_{\text{eff}} = 0$  for  $\gamma = \pi/6$ . There are, however, subleading finite-size corrections to (5.18). Similarly, the ground state for even  $L$  corresponds to the choice  $\mathbf{n} = (-1, 0, 0, +1)$  and  $\mathbf{m} = (0, 0, 0, 0)$  which results in the same effective central charge, although there are logarithmic corrections of the finite-size gap. More generally, the finite-size energies of states within the same spin and charge sector and furthermore  $n_1^+ - n_1^- = n_2^+ - n_2^-$  differ by multiples of  $K(L)$  only. For example, the finite-size estimators for the scaling dimensions  $X(L) = L(E(L) - L\varepsilon_\infty^{(B)})/(2\pi v_B) + 1/3$  of the following configurations (note that the  $N_a^\pm$  are integers, so the configurations can be realized for  $L$  even *or* odd only!)

$N_1^+$	$N_1^-$	$N_2^+$	$N_2^-$	$\mathbf{n}$	$\mathbf{m}$	$X_{\mathbf{n}}^{\mathbf{m}}$
$(L+1)/2$	$(L+1)/2$	$(L-1)/2$	$(L-1)/2$	$(-\frac{1}{2}, -\frac{1}{2}, \frac{1}{2}, \frac{1}{2})$	$(0, 0, 0, 0)$	$\frac{1}{2} - \frac{\gamma}{\pi}$
$(L+2)/2$	$L/2$	$L/2$	$(L-2)/2$	$(-1, 0, 0, 1)$	$(0, 0, 0, 0)$	$\frac{1}{2} - \frac{\gamma}{\pi} + K(L)$
$(L+3)/2$	$(L-1)/2$	$(L+1)/2$	$(L-3)/2$	$(-\frac{3}{2}, \frac{1}{2}, -\frac{1}{2}, \frac{3}{2})$	$(0, 0, 0, 0)$	$\frac{1}{2} - \frac{\gamma}{\pi} + 4K(L)$
$(L+4)/2$	$(L-2)/2$	$(L+2)/2$	$(L-4)/2$	$(-2, 1, -1, 2)$	$(0, 0, 0, 0)$	$\frac{1}{2} - \frac{\gamma}{\pi} + 9K(L)$
$L/2$	$(L-2)/2$	$(L-2)/2$	$L/2$	$(0, 1, 1, 0)$	$(0, 0, 0, 0)$	$\frac{1}{2} + \frac{\gamma}{\pi}$
$(L-1)/2$	$(L-1)/2$	$(L-1)/2$	$(L-1)/2$	$(\frac{1}{2}, \frac{1}{2}, \frac{1}{2}, \frac{1}{2})$	$(\frac{1}{2}, -\frac{1}{2}, -\frac{1}{2}, \frac{1}{2})$	$\frac{1}{2} + \frac{\gamma}{\pi}$

extrapolate to the same values  $\frac{1}{2} - \frac{\gamma}{\pi}$  and  $\frac{1}{2} + \frac{\gamma}{\pi}$ , respectively. The splitting of these levels for finite  $L$  and in particular the fine structure of gaps between the first four levels reflecting the  $L$ -dependence of  $K(L)$  is shown for  $\gamma = 2\pi/7$  in Figure 4. It is clearly seen that this fine structure in the multiplet  $X_{\mathbf{n}}^{\mathbf{n}} \rightarrow \frac{1}{2} - \frac{\gamma}{\pi}$  is very different from the corrections to scaling depending on the parity of the system size as observed between the two states shown for the multiplet  $X_{\mathbf{n}}^{\mathbf{n}} \rightarrow \frac{1}{2} + \frac{\gamma}{\pi}$ .

### The logarithmic fine structure

Our numerical results show that the low lying levels of the mixed superspin chain can be combined into groups with the same finite-size behaviour in the thermodynamic limit. For large

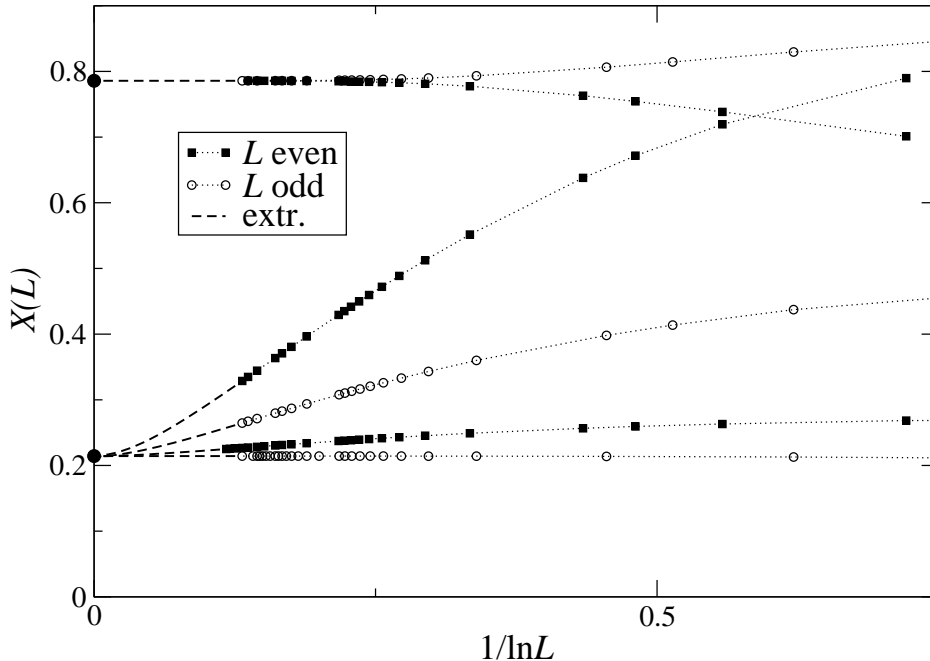


FIG. 4. Finite-size estimators for the scaling dimensions of some low lying states of the mixed superspin chain for  $\gamma = 2\pi/7$  and  $\gamma b = \pi/4$ . The lowest states extrapolate to  $\frac{1}{2} - \frac{\gamma}{\pi} = \frac{3}{14}$  and differ by multiples of  $1/(\ln L)^2$ . The other states extrapolate to  $\frac{1}{2} + \frac{\gamma}{\pi} = \frac{11}{14}$  without logarithmic corrections. Dashed lines are rational function extrapolations of the numerical data to  $L \rightarrow \infty$ .

but finite chains, however, these degeneracies are lifted and gaps  $L\Delta E \sim 1/(\ln L)^2$  appear. Such logarithmic corrections to the scaling are usually understood as a consequence of the presence of marginal operators in the spectrum of a conformal field theory [40]. In the present model there are several such operators: first, the fact that charge and spin excitations are described by bosons which are dual to each other,  $R_c^2 + R_s^2 = 2$ , gives rise to composite operators which have scaling dimension (6.13)  $X = 2$ . As has been discussed for phases A1 and A2 above, such operators are also present in the low energy sector of the model for  $b < \frac{1}{2}$  where no signs of logarithmic corrections to scaling have been observed. Here, however, the mode with vanishing coupling constant appears together with a compact self-dual boson with  $(R_3)^2 = 2$  independent of the deformation parameter  $\gamma$ . The presence of these two modes, which are not related to the physical  $U(1)$  symmetries of the  $U_q[sl(2|1)]$  mixed superspin chain, may be responsible for both the massive degeneracies of the low-lying levels in the thermodynamic limit and the presence of logarithmic corrections in the finite-size spectrum for large but finite systems.

An alternative scenario has been put forward by Ikhlef *et al.* [6] in the context of the ferromagnetic staggered six-vertex model: based on numerical evidence and supported by arguments from

an RG analysis of a supersphere sigma model they interpret the finite-size spectrum (5.17) as a signature of the emergence of a non-compact boson in the effective field theory of the model. As a consequence the coupling constant should approach its long-distance value as

$$K(L) \simeq A [B + \ln L]^{-p} \quad (5.19)$$

where  $A$  and  $B$  are functions of the system parameters and the exponent can take values  $p = 1, 2$ . The numerical data of Ref. 6 for the ferromagnetic staggered XXZ model with  $\gamma < \pi/2$  and  $b = \pi/4\gamma$  as well as our own results are consistent with this proposal for  $p = 2$  and  $A(\gamma) = 5\gamma/(\pi - 2\gamma)$ . Eq. (5.19) also agrees with what has been observed in the low energy spectrum of the antiferromagnetic superspin chain based on alternating quark and antiquark representations of  $U_q[sl(2|1)]$  [5, 17], although the amplitude  $A$  displays a different  $\gamma$ -dependence in that model.

### C. Phase B: critical theory for $\frac{1}{2} < b < \pi/4\gamma$

As mentioned above, the fact that the bare densities  $\rho_0(\lambda)$  of the  $(1, +)$ -strings (5.6) are not positive definite for  $\frac{1}{2} < b < \pi/4\gamma$  requires special attention. To find the ground state within the configurations (5.1) the energy density has to be minimized by varying the support of the root densities  $\rho^{(a)}$  (or  $\sigma^{(a)}$ ). In the integral equations (5.7) this amounts to changing the boundaries of integration to finite values.

Here we argue, however, that (5.10) does in fact describe the true thermodynamic ground state of the mixed superspin chain based on the following observations:

1. solving the integral equations (5.7) with finite boundaries numerically we find that (5.12) is a lower bound for the energy density.
2. the ground state energies obtained by exact diagonalization of the superspin chain Hamiltonian up to  $L = 4$ , i.e. 8 sites, are reproduced from the Bethe ansatz. The root configurations are consistent with the thermodynamic results.
3. the level crossings among the low energy states obtained from the Bethe ansatz for configurations with given numbers  $N_a^\pm$  of roots support the result (5.11), see Fig.5.

Based on these findings we conjecture that the critical exponents are given by (5.15) throughout the B phase. As  $b$  is varied away from the self-dual line  $\gamma b = \pi/4$ , however, the numbers  $n_a^\pm$  have to be measured relatively to the state with densities given by (5.11), i.e.

$$n_a^+ = L \left( \frac{\pi - \gamma(2b + 1)}{\pi - 2\gamma} \right) - N_a^+, \quad n_a^- = L \left( \frac{\gamma(2b - 1)}{\pi - 2\gamma} \right) - N_a^-. \quad (5.20)$$

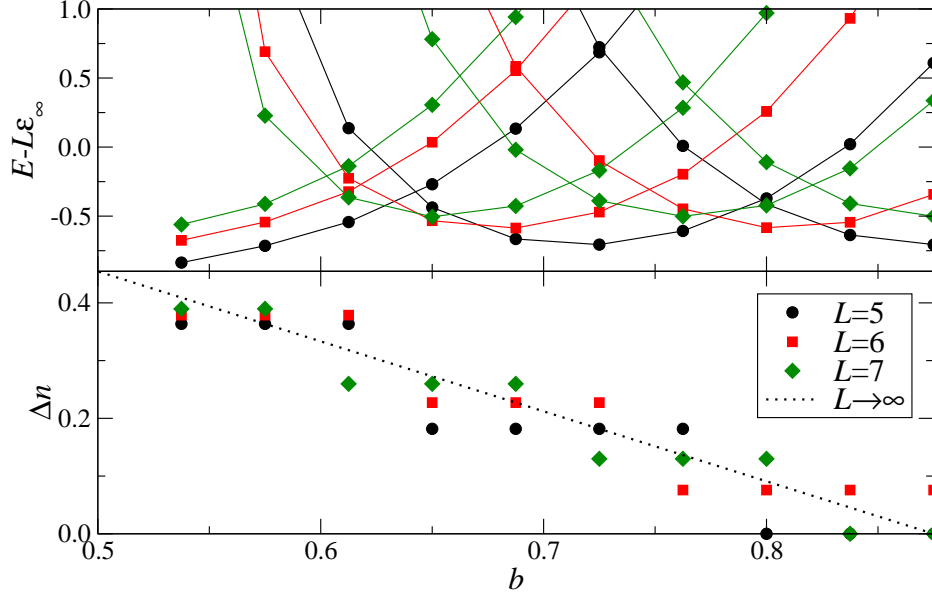


FIG. 5. Crossings of lowest levels in the  $(N_1, N_2) = (L+1, L-1)$  sectors of the mixed superspin chain (upper panel) and differences in ground state string densities  $\Delta n = (N_a^+ - N_a^-)/2L$  (lower panel) as function of the staggering parameter  $b$  for  $L = 5, 6, 7$ . The dotted line is the result (5.11) from the thermodynamic limit.

The selection rule (5.16) for the vorticities  $m_a^\pm$  remains unchanged. The quantum numbers  $n_a^\pm$ , on the other hand, take values depending on the staggering  $b$ . In the scaling dimensions (5.15), however, this affects *only* the contribution proportional to  $K(L)$ : according to (5.20) the numbers of spin and charge excitations, i.e.  $n_1^+ + n_1^- + n_2^+ + n_2^-$  and  $n_1^+ + n_1^- - n_2^+ - n_2^-$ , as well as the occupation number of the third compact boson  $n_1^+ - n_1^- - n_2^+ + n_2^-$  continue to be integers.

To verify this conjecture we have studied the finite-size scaling of the ground states for  $\gamma = 2\pi/7$  and  $b = (\pi + \gamma)/6\gamma = 3/4$  and  $b = (\pi + 2\gamma)/8\gamma = 11/16$ . As before one of the ground states is in the  $(N_1, N_2) = (L+1, L-1)$  sector but according to (5.11) the ratios  $N_a^+/N_a^-$  are 2 and 3, respectively. Depending on the system size  $L$  the root configurations and corresponding conformal dimensions according to (5.15) are for  $b = 3/4$

$N_1^+$	$N_1^-$	$N_2^+$	$N_2^-$	$\mathbf{n}$	$\mathbf{m}$	$X_{\mathbf{n}}^{\mathbf{m}}$
$(2L+3)/3$	$L/3$	$2L/3$	$(L-3)/3$	$(-1, 0, 0, 1)$	$(0, 0, 0, 0)$	$\frac{1}{2} - \frac{\gamma}{\pi} + K(L)$
$(2L+1)/3$	$(L+2)/3$	$(2L-2)/3$	$(L-1)/3$	$(-\frac{1}{3}, -\frac{2}{3}, \frac{2}{3}, \frac{1}{3})$	$(0, 0, 0, 0)$	$\frac{1}{2} - \frac{\gamma}{\pi} + \frac{1}{9}K(L)$
$(2L+2)/3$	$(L+1)/3$	$(2L-1)/3$	$(L-2)/3$	$(-\frac{2}{3}, -\frac{1}{3}, \frac{1}{3}, \frac{2}{3})$	$(0, 0, 0, 0)$	$\frac{1}{2} - \frac{\gamma}{\pi} + \frac{1}{9}K(L)$

and for  $b = 11/16$ :

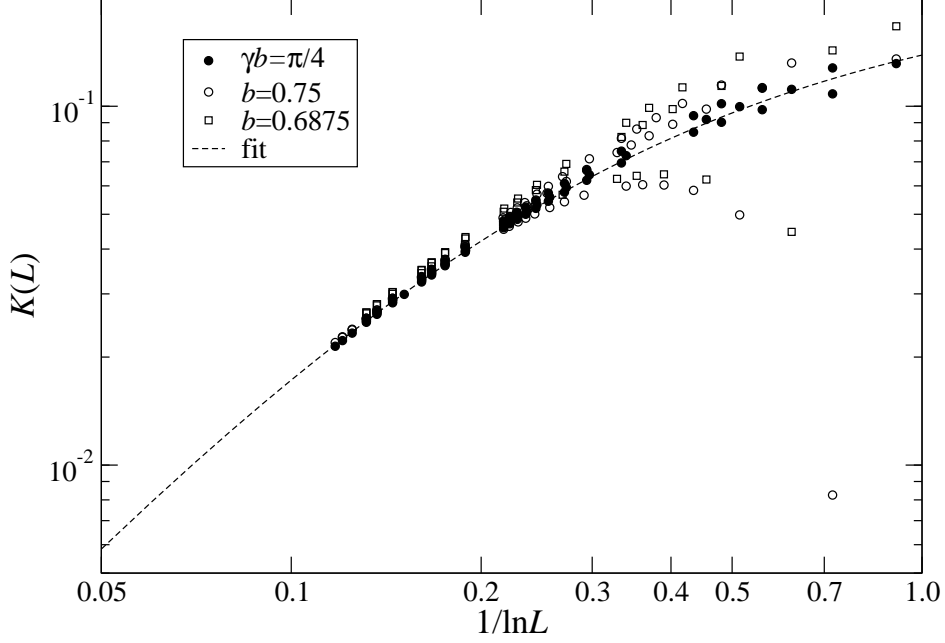


FIG. 6. Coupling constant  $K(L)$  extracted from the finite-size behaviour (5.15) of the lowest states in the  $(N_1, N_2) = (L+1, L-1)$  sectors of the mixed superspin chain for  $\gamma = 2\pi/7$  and  $b = 0.75$  and  $0.6875$ . The dashed line is a fit of (5.19) with  $p = 2$  and  $A(\gamma) = 5\gamma/(\pi - 2\gamma)$  to the data for the self-dual case  $b = \pi/4\gamma$ .

$N_1^+$	$N_1^-$	$N_2^+$	$N_2^-$	<b>n</b>	<b>m</b>	$X_{\mathbf{n}}^{\mathbf{m}}$
$(3L+4)/4$	$L/4$	$3L/4$	$(L-4)/4$	$(-1, 0, 0, 1)$	$(0, 0, 0, 0)$	$\frac{1}{2} - \frac{\gamma}{\pi} + K(L)$
$(3L+1)/4$	$(L+3)/4$	$(3L-3)/4$	$(L-1)/4$	$(-\frac{1}{4}, -\frac{3}{4}, \frac{3}{4}, \frac{1}{4})$	$(0, 0, 0, 0)$	$\frac{1}{2} - \frac{\gamma}{\pi} + \frac{1}{4}K(L)$
$(3L+2)/4$	$(L+2)/4$	$(3L-2)/4$	$(L-2)/4$	$(-\frac{1}{2}, -\frac{1}{2}, \frac{1}{2}, \frac{1}{2})$	$(0, 0, 0, 0)$	$\frac{1}{2} - \frac{\gamma}{\pi}$
$(3L+3)/4$	$(L+1)/4$	$(3L-1)/4$	$(L-3)/4$	$(-\frac{3}{4}, -\frac{1}{4}, \frac{1}{4}, \frac{3}{4})$	$(0, 0, 0, 0)$	$\frac{1}{2} - \frac{\gamma}{\pi} + \frac{1}{4}K(L)$

In Figure 6 our results for the coupling constant  $K(L)$  as extracted from the numerical data for these parameters are presented together with the ones obtained from the ground state energies of self-dual model (see Fig. 4) and a fit of the conjecture (5.19) with  $p = 2$  and  $A(\gamma) = 5\gamma/(\pi - 2\gamma)$ : from these data we conclude that the amplitude  $A(\gamma, b)$  of the coupling constant is independent of the staggering parameter  $b$ .

This would imply that the parameter  $b$  is irrelevant as far as the compactified bosonic degrees of freedom are concerned, while it acts as some kind of twist in the mode with vanishing coupling constant.

Approaching the limit  $b \rightarrow \frac{1}{2} + 0$  from above the densities  $\sigma^{(a)}(\lambda)$  of  $(1, -)$  strings vanish as does the corresponding Fermi velocity. On the line  $b = \frac{1}{2}$  the critical theory has central charge  $c = -1$  with the operator content given in Section IV B and also in Ref. 17 before.

## VI. THE *ANTI-FERROMAGNETIC* MIXED SUPERSPIN CHAIN ON THE SELF-DUAL LINE

Our numerical analysis of the Hamiltonian (2.11) for small lattice sizes indicates that the ground state of the anti-ferromagnetic superspin chain sits in the sectors  $(N_1, N_2) = (L \pm 1, L \pm 1)$  corresponding to charge zero and spin  $S_3 = \pm 1$  for parameters  $0 < \gamma < \pi/2$  and  $\gamma b = \pi/4$ , i.e. on the self-dual line. For  $L$  odd the spectrum displays this double degeneracy while we observe a four-fold degenerate ground state for  $L$  even. For these parameters we have identified the root configurations corresponding to low lying states solving the Bethe equations (2.10): apart from strings (4.1) we find roots located on the lines  $\text{Im}(\lambda) = \pm \gamma b$  which in fact dominate the low energy states. As an example, the ground state configuration of the anti-ferromagnetic mixed superspin chain on the self-dual line is given in terms of composites combining roots from both levels of the Bethe ansatz as

$$\lambda_m^{(1)} = \left(\lambda_m^{(2)}\right)^* = \lambda_m \pm i\gamma b, \quad (6.1)$$

with real center  $\lambda_m \in \mathbb{R}$ .

These configurations continue to exist away from the self-dual line. It turns out, however, that for finite chains and generic  $\frac{1}{2} < b < \pi/4\gamma$  the imaginary parts of these roots deviate from the asymptotic values  $\pm \gamma b$  by corrections which vanish as the system size  $L \rightarrow \infty$ . In the limit  $b \rightarrow \frac{1}{2}$  the ' $b$ -strings' (6.1) turn into the strange 2-string configurations describing the low-lying states of the anti-ferromagnetic  $3 \otimes \bar{3}$  superspin chain before [5, 17]. Away from  $b = \frac{1}{2}$ , however, the numerical data indicate that these states are not in the low energy sector of the model any more. Instead there appears to be a crossover to different  $b$ -dependent ground states.

Therefore we are going to concentrate our investigation of the anti-ferromagnetic superspin chain (2.11) for  $b > \frac{1}{2}$  on the self-dual case: here the additional root configurations discussed above become exact, i.e. with imaginary parts  $\equiv \pm i\pi/4$  independent of the system size  $L$ . This allows to describe most of the low energy states by the structure

$$\left\{\lambda_j^{(a)}\right\}_{j=1}^{N_a} \equiv \left\{\mu_j^{(a,+)} - i\frac{\pi}{4}\right\}_{j=1}^{N_a^+} \cup \left\{\mu_j^{(a,-)} + i\frac{\pi}{4}\right\}_{j=1}^{N_a^-}, \quad a = 1, 2, \quad \text{for } b\gamma = \pi/4 \quad (6.2)$$

where  $\mu_j^{(a,\pm)} \in \mathbb{R}$  and  $N_a = N_a^+ + N_a^-$  for  $a = 1, 2$ . We shall now use this fact to employ the analytical tools of the previous sections to start our investigations of the thermodynamic limit and finite-size properties of the anti-ferromagnetic mixed superspin chain on the self-dual line. It is convenient to shift the rapidities  $\mu_j^{(a,\pm)}$  as follows

$$\mu_j^{(a,\pm)} = \xi_j^{(a,\pm)} + i\pi/4, \quad a = 1, 2. \quad (6.3)$$



Substituting (6.3) into the Bethe equations (2.10) and taking their logarithms we find that the resulting equations for  $\xi_j^{(a,\pm)}$  are

$$\begin{aligned} L\Phi(2\xi_j^{(1,\pm)}, \gamma) &= 2\pi Q_j^{(1,\pm)} + \sum_{k=1}^{N_2^\pm} \Phi(\xi_j^{(1,\pm)} - \xi_k^{(2,\pm)}, \gamma) - \sum_{k=1}^{N_2^\mp} \Psi(\lambda_j^{(1,\pm)} - \mu_k^{(2,\mp)}, \gamma), \quad j = 1, \dots, N_1^\pm, \\ L\Phi(2\xi_j^{(2,\pm)}, \gamma) &= 2\pi Q_j^{(2,\pm)} + \sum_{k=1}^{N_1^\pm} \Phi(\xi_j^{(2,\pm)} - \xi_k^{(1,\pm)}, \gamma) - \sum_{k=1}^{N_1^\mp} \Psi(\lambda_j^{(2,\pm)} - \mu_k^{(1,\mp)}, \gamma), \quad j = 1, \dots, N_2^\pm. \end{aligned} \quad (6.4)$$

The functions  $\Phi(x, y)$  and  $\Psi(x, y)$  have been defined in Eqs. (4.3) and (4.18) above. The quantum numbers  $Q_j^{(a,\pm)}$  define the many possible branches of the logarithm and uniquely characterize an eigenstate of the system. They have to be chosen integer or half-odd integer according to the parities of the numbers  $N_a^\pm$ :

$$Q_j^{(1,\pm)} \equiv \frac{L + N_2^\pm}{2} \pmod{1}, \quad Q_j^{(2,\pm)} \equiv \frac{L + N_1^\pm}{2} \pmod{1}. \quad (6.5)$$

Note that as in phase A2 there exist root configurations with one or more roots located at  $\pm\infty$  (see also Appendix B). To deal with such configurations one can follow the above procedure to obtain equations for the finite roots *after* taking into account the infinite one(s) explicitly.

### A. Thermodynamic limit

As before we begin our analysis of the thermodynamic limit by introducing counting functions for the rapidities  $\xi_j^{(a,\pm)}$

$$\begin{aligned} z^{(1,\pm)}(\xi) &= \frac{1}{2}\Phi(2\xi, \gamma) - \frac{1}{2L} \sum_{k=1}^{N_2^\pm} \Phi(\xi - \xi_k^{(2,\pm)}, \gamma) + \frac{1}{2L} \sum_{k=1}^{N_2^\mp} \Psi(\xi - \xi_k^{(2,\mp)}, \gamma), \\ z^{(2,\pm)}(\lambda) &= \frac{1}{2}\Phi(2\xi, \gamma) - \frac{1}{2L} \sum_{k=1}^{N_1^\pm} \Phi(\xi - \xi_k^{(1,\pm)}, \gamma) + \frac{1}{2L} \sum_{k=1}^{N_1^\mp} \Psi(\xi - \xi_k^{(1,\mp)}, \gamma), \end{aligned} \quad (6.6)$$

When  $L \rightarrow \infty$  the roots  $\xi_j^{(a,\pm)}$  tend towards a continuous distribution and the derivatives of the counting functions define the corresponding densities of particles  $\sigma^{(a,\pm)}(\xi)$  and holes  $\sigma_h^{(a,\pm)}(\xi)$ , namely

$$2\pi \left( \sigma^{(a,\pm)}(\xi) + \sigma_h^{(a,\pm)}(\xi) \right) = \frac{dz^{(a,\pm)}(\xi)}{d\xi}. \quad (6.7)$$

For the ground state, the counting functions are dominated by the particle densities and Eqs. (6.4) turn into the following coupled integral relations for the densities  $\sigma^{(a,\pm)}(\xi)$ ,

$$\begin{pmatrix} \sigma^{(1,+)}(\xi) \\ \sigma^{(1,-)}(\xi) \\ \sigma^{(2,+)}(\xi) \\ \sigma^{(2,-)}(\xi) \end{pmatrix} = \frac{1}{4\pi} \begin{pmatrix} \Phi'(2\xi, \gamma) \\ \Phi'(2\xi, \gamma) \\ \Phi'(2\xi, \gamma) \\ \Phi'(2\xi, \gamma) \end{pmatrix} - \int_{-\infty}^{\infty} d\mu \mathbb{K}(\xi - \mu) \begin{pmatrix} \sigma^{(1,+)}(\mu) \\ \sigma^{(1,-)}(\mu) \\ \sigma^{(2,+)}(\mu) \\ \sigma^{(2,-)}(\mu) \end{pmatrix} \quad (6.8)$$

where the kernel matrix  $\mathbb{K}(\lambda)$  has been defined in Eq. (5.8) above. As a consequence of the fact that Eqs. (6.8) are invariant under the exchanges  $1 \leftrightarrow 2$  and  $+\leftrightarrow -$  all the densities  $\sigma^{(a,\pm)}(\xi)$  are the same. The remaining scalar integral equation can be solved by standard Fourier methods giving

$$\sigma^{(a,\pm)}(\xi) = \frac{1}{4\gamma \cosh(\frac{\pi\xi}{\gamma})}, \quad a = 1, 2. \quad (6.9)$$

Using (6.9) in (2.12) we obtain the energy density of this eigenstate of the anti-ferromagnetic superspin chain on the self-dual line  $\gamma b = \pi/4$

$$\epsilon_{\infty}^{(C)} = -2 \int_{-\infty}^{\infty} d\omega \frac{\sinh((\pi - 2\gamma)\omega/4)}{\sinh(\pi\omega/4) \cosh(\gamma\omega/2)}. \quad (6.10)$$

Starting from this state we find that there are four branches of low energy excitations with linear dispersion. Their Fermi velocity is

$$v_C = \frac{\pi}{\gamma}. \quad (6.11)$$

## B. Critical theory of the self-dual anti-ferromagnetic superspin chain

### *Finite-size spectrum*

Similar as for phase B we can employ the standard techniques to compute the finite-size scaling behaviour of the low-energy excitations and find that the energy gaps are given by

$$E(L, \gamma) - L\varepsilon_{\infty}^{(C)}(\gamma) = \frac{2\pi v_C}{L} \left[ -\frac{1}{3} + X_{n_1^+, n_1^-, n_2^+, n_2^-}^{m_1^+, m_1^-, m_2^+, m_2^-}(\gamma) \right] + o(L^{-1}). \quad (6.12)$$

where the scaling dimensions  $X_{n_1^+, n_1^-, n_2^+, n_2^-}^{m_1^+, m_1^-, m_2^+, m_2^-}(\gamma)$  associated to the four possible gapless modes are given by,

$$\begin{aligned} X_{n_1^+, n_1^-, n_2^+, n_2^-}^{m_1^+, m_1^-, m_2^+, m_2^-}(\gamma) = & \frac{\gamma}{4\pi} (n_1^+ + n_1^- - n_2^+ - n_2^-)^2 + \frac{\pi}{16\gamma} (m_1^+ + m_1^- - m_2^+ - m_2^-)^2 \\ & + \frac{\pi - 2\gamma}{8\pi} (n_1^+ + n_1^- + n_2^+ + n_2^-)^2 + \frac{\pi}{8(\pi - 2\gamma)} (m_1^+ + m_1^- + m_2^+ + m_2^-)^2 \\ & + \frac{1}{8} (n_1^+ - n_1^- + n_2^+ - n_2^-)^2 + \frac{1}{8} (m_1^+ - m_1^- + m_2^+ - m_2^-)^2 \\ & + \frac{K(L)}{8} (n_1^+ - n_1^- - n_2^+ + n_2^-)^2 + \frac{1}{8K(L)} (m_1^+ - m_1^- - m_2^+ + m_2^-)^2. \end{aligned} \quad (6.13)$$

Excitations are labeled again by charge indices  $n_a^\pm = L/2 - N_a^\pm$ ,  $a = 1, 2$  and corresponding vorticities  $m_a^\pm$ . From the constraint (6.5) that they are linked to the parities of  $n_a^\pm$  by

$$m_a^\pm = \frac{1}{2} (n_1^\pm + n_2^\pm + 1) \mod 1, \quad a = 1, 2. \quad (6.14)$$

Similar to the discussion of the finite-size spectrum in phase B three of the elementary critical modes contributing to (6.13) can be identified as free bosons: the modes corresponding to spin and charge excitations have compactification radii depending on the deformation parameter as  $R_c^2 = 4\gamma/\pi = 2 - R_s^2$ , i.e. they are interchanged as compared to what has been found in the ferromagnetic regime B. As in that phase there is a third compact boson which cannot be identified with the  $U(1)$  charges of the superspin chain, its radius takes the self-dual value  $(R_3)^2 = 2$  independent of  $\gamma$ . Again, the finite-size behaviour of the fourth mode cannot be studied within this approach: as a consequence of the singular kernel of the Bethe ansatz integral equations one only finds that the corresponding coupling constant  $K(L)$  vanishes in the thermodynamic limit. This implies that states with  $n_1^+ - n_1^- - n_2^+ + n_2^- = 0$  are degenerate to order  $L^{-1}$  and only states with  $m_1^+ - m_1^- - m_2^+ + m_2^- = 0$  appear in the low energy spectrum.

A preliminary verification of the above proposal (6.13) can be easily done by considering the subsector associated to the staggered six-vertex model. In this case we have the same charge and vorticity indices for both levels  $a = 1, 2$ . Taking into account the relation (3.10) between the spectra of the mixed superspin chain and the staggered XXZ model and setting  $n_1^\pm = n_2^\pm = n^\pm$ ,  $m_1^\pm = m_2^\pm = m^\pm$  in (6.13) we find

$$\begin{aligned} E^{(6v)}(L, \gamma) - \frac{L}{2} \varepsilon_\infty^{(C)}(\gamma) = & \frac{2\pi v_C}{L} \left[ -\frac{1}{6} + \tilde{X}_{n^+, n^-}^{m^+, m^-}(\gamma) \right] + o(L^{-1}), \\ \tilde{X}_{n^+, n^-}^{m^+, m^-}(\gamma) = & \frac{(\pi - 2\gamma)}{4\pi} (n^+ + n^-)^2 + \frac{\pi}{4(\pi - 2\gamma)} (m^+ + m^-)^2 \\ & + \frac{1}{4} (n^+ - n^-)^2 + \frac{1}{4} (m^+ - m^-)^2. \end{aligned} \quad (6.15)$$

From (6.15) we see that the modes associated to the amplitude  $K(L)$  do not contribute to the spectrum of the staggered six-vertex model. The conformal dimensions  $\tilde{X}_{n^+, n^-}^{m^+, m^-}(\gamma)$  are in accordance with those proposed recently in Ref. 41.

### Numerical results

From the exact diagonalization of the mixed superspin chain for small  $L$  we have identified the ground state to be located in the sectors  $(N_1, N_2) = (L \pm 1, L \pm 1)$ . Following the selection rules for the  $n_a^\pm, m_a^\pm$  given above, the lowest level is given by  $\mathbf{n} \equiv (n_1^+, n_1^-, n_2^+, n_2^-) = (\frac{1}{2}, \frac{1}{2}, \frac{1}{2}, \frac{1}{2})$  for  $L$  odd and  $\mathbf{n} = (0, 1, 1, 0)$  for  $L$  even while  $\mathbf{m} \equiv (m_1^+, m_1^-, m_2^+, m_2^-) = (0, 0, 0, 0)$  in both cases. According to (6.12) the ground state energy scales as

$$\begin{aligned} E_0(L, \gamma) - L\varepsilon_\infty^{(C)}(\gamma) &= -\frac{\pi v_C}{6L} \left[ 2\frac{6\gamma - \pi}{\pi} \right] + o(L^{-1}), \quad \text{for } L \text{ odd} \\ &= -\frac{\pi v_C}{6L} \left[ 2\frac{6\gamma - \pi}{\pi} \right] + \frac{2\pi v_C}{L} \left[ \frac{1}{2}K(L) \right] + o(L^{-1}), \quad \text{for } L \text{ even}. \end{aligned} \quad (6.16)$$

Note that the ground state of the odd  $L$  superspin chains is also in the XXZ subsector of this model. As mentioned above,  $K(L) \rightarrow 0$  for  $L \rightarrow \infty$ , therefore we find an effective central charge  $c_{\text{eff}} = 2(6\gamma - \pi)/\pi$  in both cases. Upon fine-tuning of the deformation parameter to  $\gamma = \pi/6$  the ground state energy of the mixed superspin chain is exactly  $L\varepsilon_\infty^{(C)}(\gamma)$  without subleading corrections, i.e.  $c_{\text{eff}} = 0$ . It turns out that there is a family of states in this sector with finite-size gap to the ground states (6.16) vanishing as multiples of  $K(L)$ : the lowest energy in the sector  $N_1^+ = N_2^- = (L - 1 + \ell)/2$  and  $N_1^- = N_2^+ = (L - 1 - \ell)/2$  with  $\ell = 0, \pm 1, \pm 2, \dots$  is degenerate with the ground state (note that  $N_a^\pm$  are integers, therefore only configurations with even (odd)  $\ell$  can be realized for odd (even)  $L$ ). In Figure 7 the splitting of the levels with

$N_1^+$	$N_1^-$	$N_2^+$	$N_2^-$	$\mathbf{n}$	$\mathbf{m}$	$X_{\mathbf{n}}^{\mathbf{m}}$
$(L-1)/2$	$(L-1)/2$	$(L-1)/2$	$(L-1)/2$	$(\frac{1}{2}, \frac{1}{2}, \frac{1}{2}, \frac{1}{2})$	$(0, 0, 0, 0)$	$\frac{1}{2} - \frac{\gamma}{\pi}$
$L/2$	$(L-2)/2$	$(L-2)/2$	$L/2$	$(0, 1, 1, 0)$	$(0, 0, 0, 0)$	$\frac{1}{2} - \frac{\gamma}{\pi} + \frac{1}{2}K(L)$
$(L+1)/2$	$(L-3)/2$	$(L-3)/2$	$(L+1)/2$	$(-\frac{1}{2}, \frac{3}{2}, \frac{3}{2}, -\frac{1}{2})$	$(0, 0, 0, 0)$	$\frac{1}{2} - \frac{\gamma}{\pi} + 2K(L)$

as a function of the system size is shown for  $\gamma = 2\pi/7$ ,  $\gamma b = \pi/4$ . The gaps between the lowest levels vanish for  $L \rightarrow \infty$ , similarly as has been found in phase B above. Based on the proposal (5.19) we can analyze the behaviour of the coupling constant  $K(L)$  appearing in the scaling dimensions of the mixed superspin chain. We have used the numerical data for the ground state energy of the even  $L$  chains to extract  $K(L)$ . Comparing  $K(L)$  with  $K(L/2)$  we obtain estimates for the amplitude

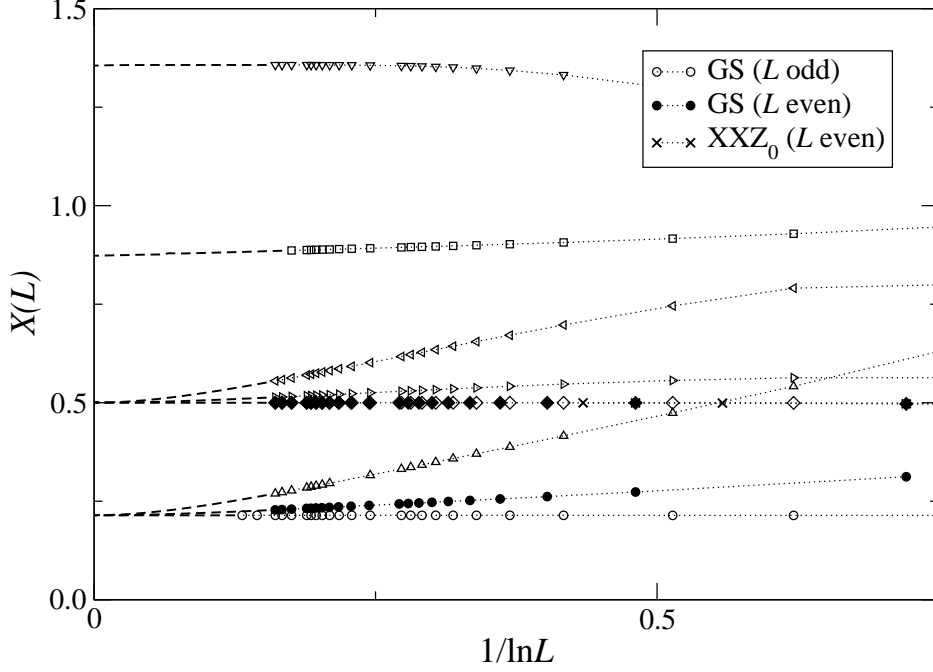


FIG. 7. Finite-size estimators  $X(L) = L(E(L) - L\varepsilon_\infty^{(C)})/(2\pi v_C) + 1/3$  for the scaling dimensions of some low lying states of the anti-ferromagnetic mixed superspin chain for  $\gamma = 2\pi/7$  on the self-dual line  $\gamma b = \pi/4$ . Dimensions appearing for odd (even)  $L$  are shown as open (filled) symbols. The scaling dimensions of the lowest states extrapolate to  $\frac{1}{2} - \frac{\gamma}{\pi} = \frac{3}{14}$  and  $\frac{1}{2}$  but differ by multiples of  $K(L)$ . The other levels displayed in the figure extrapolate to  $\frac{\pi}{4\gamma} = \frac{7}{8}$  and  $\frac{5}{2} - \frac{4\gamma}{\pi} = \frac{19}{14}$ , respectively. Dashed lines are rational function extrapolations of the numerical data to  $L \rightarrow \infty$ .

$A(\gamma)$  for various values of the deformation parameter. As shown in Table XIII the proposal (5.19) does describe the data quite well with

$$A(\gamma, b = \pi/4\gamma) = 5 \frac{\pi - 2\gamma}{4\gamma}. \quad (6.17)$$

A second group of states with scaling dimensions extrapolating to  $X(\gamma) = \frac{1}{2}$  independent of  $\gamma$  presented in Figure 7 is given by the following configurations:

$N_1^+$	$N_1^-$	$N_2^+$	$N_2^-$	<b>n</b>	<b>m</b>	$X_{\mathbf{n}}^{\mathbf{m}}$
$L/2$	$L/2$	$(L-2)/2$	$(L-2)/2$	$(0, 0, 1, 1)$	$(0, 0, 0, 0)$	$\frac{1}{2}$
$L/2$	$L/2$	$L/2$	$L/2$	$(0, 0, 0, 0)$	$(\frac{1}{2}, -\frac{1}{2}, \frac{1}{2}, -\frac{1}{2})$	$\frac{1}{2}$
$(L+1)/2$	$(L-1)/2$	$(L-3)/2$	$(L-1)/2$	$(-\frac{1}{2}, \frac{1}{2}, \frac{3}{2}, \frac{1}{2})$	$(0, 0, 0, 0)$	$\frac{1}{2} + \frac{1}{2}K(L)$

Among these, the state corresponding to  $X_{(0,0,0,0)}^{(\frac{1}{2}, -\frac{1}{2}, \frac{1}{2}, -\frac{1}{2})}(\gamma) = \frac{1}{2}$  is the lowest state in the XXZ subsector of the model for even  $L$ , it has spin  $S_3 = 0$ .

For the mixed superspin chain two more states with this finite-size behaviour appear. They are given by configurations involving two infinite roots  $\lambda^{(1)} = -\lambda^{(2)} = \infty$  of the Bethe equations (2.10) in addition to the  $N_a^\pm$  finite ones<sup>2</sup>:

$N_1^+$	$N_1^-$	$N_2^+$	$N_2^-$	<b>n</b>	<b>m</b>	$X_{\mathbf{n}}^{\mathbf{m}}$
$(L-1)/2$	$(L-1)/2$	$(L-1)/2$	$(L-1)/2$	$(0, 0, 0, 0)$	$(\frac{1}{2}, -\frac{1}{2}, \frac{1}{2}, -\frac{1}{2})$	$\frac{1}{2}$
$(L+1)/2$	$(L-3)/2$	$(L-3)/2$	$(L+1)/2$	$(-1, 1, 1, -1)$	$(\frac{1}{2}, -\frac{1}{2}, \frac{1}{2}, -\frac{1}{2})$	$\frac{1}{2} + 2K(L)$

The finite-size estimators of the scaling dimensions for these states at  $\gamma = 2\pi/7$  are also included in Figure 7.

We have identified two more states with larger scaling dimensions: the configuration of the state with dimension  $X_{(0,0,0,0)}^{(\frac{1}{2}, \frac{1}{2}, -\frac{1}{2}, -\frac{1}{2})}(\gamma)$  contains two infinite roots  $\lambda^{(1)} = -\lambda^{(2)} = \infty$ , the one with dimension  $X_{(\frac{1}{2}, \frac{3}{2}, \frac{1}{2}, \frac{3}{2})}^{(0,0,0,0)}(\gamma)$  is an excitation within the XXZ subsector of the model. The corresponding configurations of finite roots are given by

$N_1^+$	$N_1^-$	$N_2^+$	$N_2^-$	<b>n</b>	<b>m</b>	$X_{\mathbf{n}}^{\mathbf{m}}$
$(L-1)/2$	$(L-1)/2$	$(L-1)/2$	$(L-1)/2$	$(0, 0, 0, 0)$	$(\frac{1}{2}, \frac{1}{2}, -\frac{1}{2}, -\frac{1}{2})$	$\frac{\pi}{4\gamma}$
$(L-1)/2$	$(L-3)/2$	$(L-1)/2$	$(L-3)/2$	$(\frac{1}{2}, \frac{3}{2}, \frac{1}{2}, \frac{3}{2})$	$(0, 0, 0, 0)$	$\frac{5}{2} - \frac{4\gamma}{\pi}$

To provide further evidence for the proposed  $L$ -dependence (5.19) we have extracted the coupling constant  $K(L)$  from all gaps between the levels in the groups extrapolating to  $X(\gamma) = \frac{1}{2} - \gamma/\pi$  and  $\frac{1}{2}$ , respectively. In Figure 8 we present the resulting data for  $\gamma = 2\pi/7$ ,  $b = 7/8$  together with a fit of (5.19) using  $p = 2$  and  $A(\gamma = 2\pi/7) = 15/8$  according to (6.17). Additional support for this behaviour of the coupling constant comes from a Bethe state with charge  $B = \frac{1}{2}$  and spin  $S_3 = 2$  appearing in the spectrum of the mixed superspin chain for odd  $L$ : choosing  $N_1^+ = N_1^- = N_2^+ = (L-1)/2$  and  $N_2^- = (L-3)/2$  and quantum numbers (6.5)

$$\begin{aligned} Q_j^{(1,+)} &= -\frac{L+1}{4} + j, & Q_j^{(1,-)} &= -\frac{L+3}{4} + j, \\ Q_j^{(2,+)} &= -\frac{L+1}{4} + j, & Q_j^{(2,-)} &= -\frac{L-3}{4} + j, \end{aligned} \quad (6.18)$$

( $j$  takes values  $1, \dots, N_a^\pm$  in the corresponding sequences) we have solved the Bethe equations numerically. In the thermodynamic limit this state disappears from the low energy spectrum. Therefore it plays no role for the effective field theory and it should not be expected that the finite-size analysis employed above is applicable here. Nevertheless the finite-size behaviour of this level can be described by (6.12) and (6.13) with a “scaling dimension”

$$X_{(\frac{1}{2}, \frac{1}{2}, \frac{1}{2}, \frac{3}{2})}^{(0, -\frac{1}{2}, 0, \frac{1}{2})}(\gamma) = \frac{5\pi - 4\gamma}{4\pi} + \frac{1}{8}K(L) + \frac{1}{8K(L)}. \quad (6.19)$$

<sup>2</sup> The existence of such configurations has been already established for the 2-site system, see Appendix B, and for the low energy states of the system for  $b < \frac{1}{2}$ .

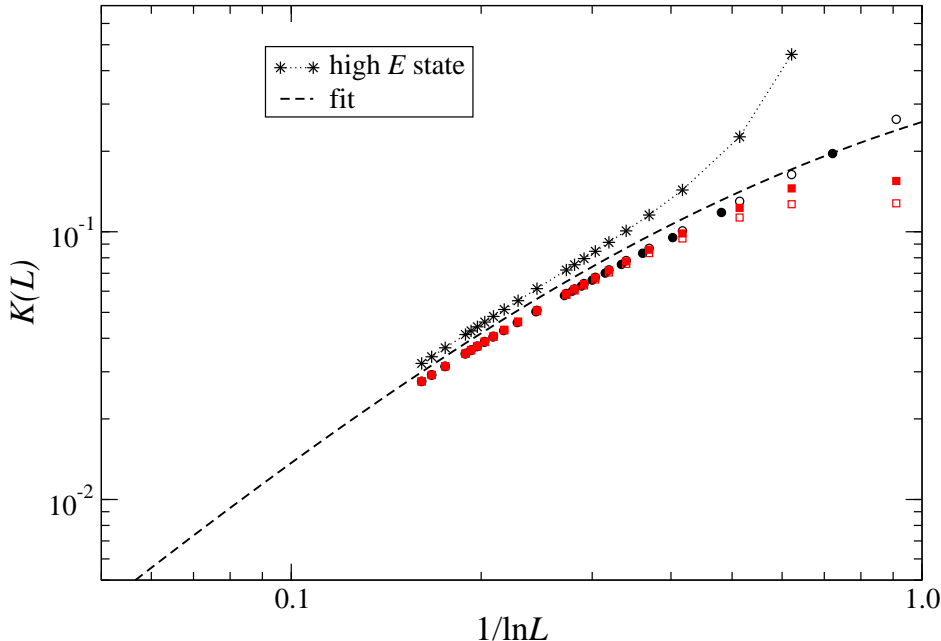


FIG. 8. Coupling constant  $K(L)$  extracted from four lying levels of the finite-size spectrum with  $X(\gamma) \rightarrow (\pi - 2\gamma)/2\pi$  (black symbols) and for  $X(\gamma) \rightarrow \frac{1}{2}$  (red symbols) for  $\gamma = 2\pi/7$  and  $b = 7/8$ . Data obtained from the high energy state with dimension (6.19) are denoted by '\*'. The dashed line is a fit of (5.19) with  $A(\gamma = 2\pi/7) = 15/8$  to the numerical data.

Using this prediction we can extract  $K(L)$  from our numerical data for this state. Surprisingly, it agrees well with what has been obtained from the logarithmic fine structure of the low-lying states before, see Figure 8.

### C. $\frac{1}{2} \leq b < \pi/4\gamma$ and connection to the $3 \otimes \bar{3}$ superspin chain

As mentioned at the beginning of this section configurations involving roots with  $Im(\lambda_j^{(a)}) \approx \pm\gamma b$  continue to exist away from the self-dual line. Restricting oneself to these configurations as in (6.2), however, does not capture the low energy part of the spectrum of the anti-ferromagnetic mixed superspin chain as  $b \rightarrow \frac{1}{2}$ . In fact, comparing (2.10) or (3.9) with the Bethe equations obtained for spin chains based on general spin- $S$  representations of  $U_q[sl(2)]$  the phase factors appearing in the Bethe equations for the present model can be identified with those arising from effective spins  $(b + \frac{1}{2})$  and  $-(b - \frac{1}{2})$ , respectively. Hence, for  $b > \frac{1}{2}$  we have a system mixing representations with different signs of the effective spin. For such a case an analysis of the thermodynamic limit based on some kind of string hypothesis is not known.

For  $b = \frac{1}{2}$ , however, some of the statistical weights (A1) appearing in the  $R$ -matrix vanish. The

remaining non-degenerate subsector of the mixed superspin chain (2.8) at  $b = \frac{1}{2}$  coincides with the spectrum of the antiferromagnetic superspin chain built from alternating three-dimensional quark  $[3]$  and antiquark  $[\bar{3}]$  representations of  $U_q[sl(2|1)]$ , see also Appendix B. The low energy spectrum of that model has been studied mostly in the zero charge sector,  $N_1 = N_2$ , in particular for root configurations consisting of the 'strange strings' [5, 17]. Under an adiabatic change of the staggering parameter from  $b = \frac{1}{2}$  to the self-dual line these configurations evolve into the  $b$ -string configurations (6.1) studied for the low energy states of the self-dual anti-ferromagnetic mixed superspin chain (2.11) above. As a consequence the resulting scaling dimensions of these states exhibit the same dependence on the deformation parameter  $\gamma$ , i.e. (6.13) for  $n_1^\pm = n_2^\mp$ , although with a different amplitude of the coupling constant  $K(L)$ . The effective central charges of the two models, however, differ: the effective central charge of the  $3 \otimes \bar{3}$  chain changes from  $c = 0$  for  $0 \leq \gamma < \pi/4$  to  $c_{\text{eff}} = 3 - 6(\pi - 2\gamma)/\pi$  for  $\pi/4 < \gamma < \pi/2$ . This should be compared to the finite-size spectrum of the present model which has  $c_{\text{eff}} = 4 - 6(\pi - 2\gamma)/\pi$  according to (6.12).

This difference can be interpreted as indication that projecting out the sector of the mixed superspin chain which degenerates as  $b = \frac{1}{2}$  removes not only the states governing the low energy sector of the model for  $b > \frac{1}{2}$  but also one of the gapless modes present in the critical theory for the self-dual line. A proof of this connection, however, would require a better understanding of the antiferromagnetic mixed superspin chain for  $\frac{1}{2} < b < \pi/4\gamma$  which is beyond of the scope of this paper.

## VII. SUMMARY & CONCLUSION

In this paper we have introduced a family of vertex models from alternating four-dimensional typical representations of the superalgebra  $U_q[sl(2|1)]$ . These models or, equivalently, the mixed superspin chains are integrable for a range of two continuous parameters  $q = e^{2i\gamma}$  related to the deformation  $b$  labelling the typical representation. We have investigated the thermodynamic limit of the model and identified the low energy effective theory which determine the critical behaviour of the model in the different parameter regions.

For  $|b| < \frac{1}{2}$  we have identified the critical theory as a  $c = -1$  conformal field theory exhibiting exact separation of spin and charge degrees of freedom. This holds for both the antiferromagnetic and ferromagnetic superspin chain or, using the identity (2.14) for the entire critical range of the deformation parameter  $0 < \gamma < \pi$ . Note that as the isotropic points  $\gamma = 0$  ( $\gamma = \pi$ ) are approached, the dispersion of the charge (spin) mode becomes non-relativistic. This agrees with



what has been found before for the antiferromagnetic  $U_q[osp(2|2)]$  chain and the ferromagnetic  $U_q[sl(2|1)]$  superspin chain with alternating three-dimensional atypical representations [16, 17]. It is also consistent with what is known for the six-vertex model hidden inside the superspin chain: here the alternation of representations in the supersymmetric model corresponds to a staggering  $\pm i\gamma b$  of the spectral parameter, see (3.1). The critical properties of spin chains resulting from such a construction with *real* staggering (implying purely imaginary  $b$ ) [42, 43] are identical to those of the homogeneous XXZ spin chain [44–46], i.e. those of a free boson compactified to a circle with radius depending on the deformation parameter.

The case  $b = \pm \frac{1}{2}$  requires special attention: for this choice of the representation parameter some of the vertex weights vanish and the Yang-Baxter equation (2.2) provides the basis for the fusion procedure allowing to construct vertex models based on higher-dimensional representations of the underlying algebra. For the present model this leads to a degeneration of the spectrum leaving the superspin chain with alternating three-dimensional quark and antiquark representations as the non-trivial sector. For the ferromagnetic superspin chain the critical behaviour on the line  $b = \frac{1}{2}$  coincides with what we have found here for  $|b| < \frac{1}{2}$  [17]. The zero-charge sector of the antiferromagnetic  $3 \otimes \bar{3}$  model has also been studied previously: starting from the XXZ spin-1 chain [23] hidden inside this sector at least part of the operator content of the critical theory has been identified [5, 17]. In addition to the compactified boson and the Ising mode of the spin-1 chain indications were found for the presence of another critical mode with unusual properties, possibly signalling the presence of a boson with non-compact target space in the spectrum of the antiferromagnetic superspin chain.

For values of the representation parameter between  $b = \frac{1}{2}$  and the self-dual line  $b = \pi/4\gamma$  we have analyzed the thermodynamic limit of the ferromagnetic mixed superspin chain based on the exact solution and supported by numerical analysis. Similar as in the phases for  $|b| < \frac{1}{2}$  the operator content does not depend on the representation parameter. The low energy spectrum, however, contains four gapless modes. Only two of these can be related to the physical degrees of freedom of the model, i.e. spin and charge. One of the remaining modes is a free boson compactified at the self-dual radius  $R^2 = 2$ , or equivalently a  $SU(2)_1$  WZW model, independent of the deformation parameter. The fourth mode has a coupling constant which vanishes in the thermodynamic limit. The spectral degeneracies are lifted for lattices of finite length  $L$  leading to a logarithmic fine structure in the spectrum of scaling dimensions. This behaviour is similar to what we have discussed above for the antiferromagnetic  $3 \otimes \bar{3}$  superspin chain. Variation of the value of the representation parameter  $b$  acts on this mode as a twist. Interestingly, this mode with vanishing coupling constant

has been observed before in model appearing as the XXZ subsector of the ferromagnetic mixed superspin chain for  $b = \pi/4\gamma$  [6, 39] which is related to the antiferromagnetic critical line of the Potts model.

For the antiferromagnetic mixed superspin chain with  $\frac{1}{2} < b \leq \pi/4\gamma$  the root configurations solving the Bethe equations (2.10) relevant for the low energy states in the thermodynamic limit have been indentified *only* on the self-dual line  $b = \pi/4\gamma$ . On this line the operator content of the critical theory has been found to be related to that of the ferromagnetic chain under the replacement  $\gamma \leftrightarrow (\pi/2) - \gamma$ . In particular, there are two critical modes in addition to the ones related to spin and charge degrees of freedom. In this regime, however, the bosonic mode with radius  $R^2 = 2$  replaces the noncompact one in the XXZ subsector. This is the reason why no logarithmic fine structure has been observed in the anisotropic critical regime of the Potts model [41].

The mixed superspin chain built from alternating a four-dimensional typical representation of the superalgebra  $U_q[sl(2|1)]$  with its dual shows an extremely rich phase diagram. Within this model other systems with ordinary symmetries and twisted boundary conditions are hidden which opens the possibility to study the peculiar critical properties found in staggered models in a larger context. There are still several open problems in the analysis of this model: most important, a basis for an analytical study of the thermodynamic properties of the antiferromagnetic model inside phase C is still lacking. The ground states for  $b = \frac{1}{2}$  and  $b = \pi/4\gamma$  can be related to each other by adiabatic variation of the representation parameter. Our numerical studies, however, provide strong evidence that the ground states and low lying excitations for intermediate values of  $b$  are not accessible this way. Another problem is the lack of an analytical derivation of the finite-size behaviour of the spectrum related to the mode with vanishing conformal weight.

The model considered here can be extended in several promising directions: first the  $\mathbb{Z}_2$  staggering of the vertex model can be generalized to obtain models with larger unit cell. In the enlarged parameter space more phases are expected to appear with boundaries related to higher-level fusion of the underlying single-row transfer matrices. Another way to realize more general phases is by building lattice models based on higher-dimensional representations of the underlying algebra. Already the homogeneous models built on the  $4S + 1$ -dimensional atypical representations of  $sl(2|1)$  display an interesting critical behaviour [47, 48]. Alternation of vertices carrying representations dual to each other and including deformation should lead to a rich phase diagram extending what is known about the critical behaviour of the higher spin XXZ models [49–52].

## ACKNOWLEDGMENTS

We thank Guiliano A. P. Ribeiro who participated in an early stage of this project. MJM has been supported in part by CAPES/DAAD grant no. 4062/11-6. Additional funding for this project has been provided by the Deutsche Forschungsgemeinschaft, the Brazilian Foundation CNPq, and the Centre for Quantum Engineering and Space-Time Research (QUEST).

### Appendix A: The Boltzmann weights

The explicit expressions for the Boltzmann weights  $a_j$ ,  $b_{jk}$ ,  $c_{jk}$  and  $d_{jk}$  appearing in the  $R$ -matrix (2.1) can be obtained from Ref. 11 after correcting a few misprints. Defining the quantum group parameter by  $q = \exp(2i\gamma)$  we find that their dependence on the four dimensional representation values  $b_1$  and  $b_2$  are,

$$\begin{aligned}
a_1 &= a_4 = -1, \quad a_2 = \frac{\sinh(i\gamma(1 - b_1 - b_2) + \lambda)}{\sinh(i\gamma(1 - b_1 - b_2) - \lambda)}, \quad a_3 = \frac{\sinh(i\gamma(1 + b_1 + b_2) + \lambda)}{\sinh(i\gamma(1 + b_1 + b_2) - \lambda)}, \\
b_{12} &= b_{42} = \frac{\sinh(i\gamma(b_1 - b_2) - \lambda)}{\sinh(i\gamma(b_1 + b_2 - 1) + \lambda)}, \quad b_{21} = b_{24} = \frac{\sinh(i\gamma(b_2 - b_1) - \lambda)}{\sinh(i\gamma(b_1 + b_2 - 1) + \lambda)}, \\
b_{13} &= b_{43} = \frac{\sinh(i\gamma(b_2 - b_1) - \lambda)}{\sinh(-i\gamma(b_1 + b_2 + 1) + \lambda)}, \quad b_{31} = b_{34} = \frac{\sinh(i\gamma(b_1 - b_2) - \lambda)}{\sinh(-i\gamma(b_1 + b_2 + 1) + \lambda)}, \\
c_{12} &= \exp(-2\lambda)c_{21} = c_{42} = \exp(-2\lambda)c_{24} = \exp(-\lambda) \frac{\sqrt{\sinh(i\gamma(2b_1 - 1)) \sinh(i\gamma(2b_2 - 1))}}{\sinh(\lambda + i\gamma(b_1 + b_2 - 1))}, \\
c_{13} &= \exp(2\lambda)c_{31} = c_{43} = \exp(2\lambda)c_{34} = \exp(\lambda) \frac{\sqrt{\sinh(i\gamma(2b_1 + 1)) \sinh(i\gamma(2b_2 + 1))}}{\sinh(i\gamma(b_1 + b_2 + 1) - \lambda)}, \\
d_{41} &= d_{14} = \frac{\sinh(i\gamma(b_1 - b_2) + \lambda) \sinh(i\gamma(b_2 - b_1) + \lambda)}{\sinh(i\gamma(b_1 + b_2 - 1) + \lambda) \sinh(i\gamma(b_1 + b_2 + 1) - \lambda)}, \\
d_{32} &= \frac{\sinh(i\gamma(b_1 - b_2) + \lambda) \sinh(i\gamma(b_1 - b_2 - 2) + \lambda)}{\sinh(i\gamma(b_1 + b_2 - 1) + \lambda) \sinh(i\gamma(b_1 + b_2 + 1) - \lambda)}, \\
d_{23} &= \frac{\sinh(i\gamma(b_2 - b_1) + \lambda) \sinh(i\gamma(b_2 - b_1 - 2) + \lambda)}{\sinh(i\gamma(b_1 + b_2 - 1) + \lambda) \sinh(i\gamma(b_1 + b_2 + 1) - \lambda)}, \\
d_{42} &= \exp(-2\lambda - 2i\gamma)d_{31} = -\exp(-2\lambda)d_{34} = -\exp(-2i\gamma)d_{12} \\
&= \exp(-\lambda - i\gamma) \frac{\sqrt{\sinh(i\gamma(2b_1 - 1)) \sinh(i\gamma(2b_2 + 1))} \sinh(i\gamma(b_1 - b_2) + \lambda)}{\sinh(i\gamma(b_1 + b_2 - 1) + \lambda) \sinh(i\gamma(b_1 + b_2 + 1) - \lambda)}, \\
d_{43} &= -\exp(2\lambda)d_{24} = -\exp(-2i\gamma)d_{13} = \exp(2\lambda - 2i\gamma)d_{21} \\
&= -\exp(\lambda - i\gamma) \frac{\sqrt{\sinh(i\gamma(2b_2 - 1)) \sinh(i\gamma(2b_1 + 1))} \sinh(i\gamma(b_2 - b_1) + \lambda)}{\sinh(i\gamma(b_1 + b_2 - 1) + \lambda) \sinh(i\gamma(b_1 + b_2 + 1) - \lambda)}, \\
d_{33} &= \exp(4\lambda)d_{22} \\
&= \exp(2\lambda) \frac{\sqrt{\sinh(i\gamma(2b_1 + 1)) \sinh(i\gamma(2b_2 + 1)) \sinh(i\gamma(2b_1 - 1)) \sinh(i\gamma(2b_2 - 1))}}{\sinh(i\gamma(b_1 + b_2 - 1) + \lambda) \sinh(i\gamma(b_1 + b_2 + 1) - \lambda)}, \\
d_{44} &= \frac{\exp(-2\lambda) \sinh(2i\gamma) + \exp(-2i\gamma) \cosh(2i\gamma(b_1 - b_2)) - \cosh(2i\gamma(b_1 + b_2))}{2 \sinh(i\gamma(b_1 + b_2 - 1) + \lambda) \sinh(i\gamma(b_1 + b_2 + 1) - \lambda)}, \\
d_{11} &= \frac{-\exp(2\lambda) \sinh(2i\gamma) + \exp(2i\gamma) \cosh(2i\gamma(b_1 - b_2)) - \cosh(2i\gamma(b_1 + b_2))}{2 \sinh(i\gamma(b_1 + b_2 - 1) + \lambda) \sinh(i\gamma(b_1 + b_2 + 1) - \lambda)}.
\end{aligned} \tag{A1}$$

## Appendix B: The two-site model

For  $L = 1$  the transfer matrices (2.3) act on a Hilbert space of dimension 16. The eigenvalues  $\Lambda^{(b,\{b,-b\})}(\lambda)$  and the corresponding Bethe roots are obtained from solutions of the Bethe equations:

- $(N_1, N_2) = (0, 0)$  – the pseudo vacuum:

$$\Lambda_{00}^{(b,\{b,-b\})}(\lambda) = \left( \frac{\sin \gamma}{\sinh(\lambda - i\gamma)} \right)^2 \frac{\sinh(2\lambda - i\gamma(2b+1)) \sinh(2\lambda + i\gamma(2b-1))}{\sinh(\lambda - i\gamma(2b+1)) \sinh(\lambda + i\gamma(2b-1))}. \quad (\text{B1})$$

This state is degenerate to the one with  $B = 0$ ,  $S_3 = -1$  due to the discrete spin inversion symmetry  $S_3 \leftrightarrow -S_3$  of the model.

- $(N_1, N_2) = (1, 0)$ :

The Bethe equation has two solutions:  $\lambda^{(1)} = 0$  giving the transfer matrix eigenvalue

$$\begin{aligned} \Lambda_{10,+}^{(b,\{b,-b\})}(\lambda) = & -4 \left( \frac{\sin \gamma}{\sinh(\lambda - i\gamma)} \right)^2 \sin(\gamma(b + \frac{1}{2})) \sin(\gamma(b - \frac{1}{2})) \\ & \times \frac{\cosh(\lambda - i\gamma(b + \frac{1}{2})) \cosh(\lambda + i\gamma(b - \frac{1}{2}))}{\sinh(\lambda - i\gamma(2b+1)) \sinh(\lambda + i\gamma(2b-1))}, \end{aligned} \quad (\text{B2})$$

and  $\lambda^{(1)} = i\pi/2$ , resulting in

$$\begin{aligned} \Lambda_{10,-}^{(b,\{b,-b\})}(\lambda) = & 4 \left( \frac{\sin \gamma}{\sinh(\lambda - i\gamma)} \right)^2 \cos(\gamma(b + \frac{1}{2})) \cos(\gamma(b - \frac{1}{2})) \\ & \times \frac{\sinh(\lambda - i\gamma(b + \frac{1}{2})) \sinh(\lambda + i\gamma(b - \frac{1}{2}))}{\sinh(\lambda - i\gamma(2b+1)) \sinh(\lambda + i\gamma(2b-1))}. \end{aligned} \quad (\text{B3})$$

Both of these eigenvalues are fourfold degenerate: first they are present in the  $S_3 = -\frac{1}{2}$  sector due to spin inversion. In addition, since the expressions (B2) and (B3) are invariant under  $b \leftrightarrow -b$  charge conjugation, the same eigenvalues in the sector  $(N_1, N_2) = (0, 1)$  for  $\lambda^{(2)} = 0$  and  $i\pi/2$ , respectively.

- $(N_1, N_2) = (2, 0)$ :

The solution to the Bethe equations is  $\lambda_1^{(1)} = 0$ ,  $\lambda_2^{(1)} = i\pi/2$  giving

$$\begin{aligned} \Lambda_{20}^{(b,\{b,-b\})}(\lambda) = & \frac{1}{2} \left( \frac{\sin \gamma}{\sinh(\lambda - i\gamma)} \right)^2 \frac{1}{\sinh(\lambda - i\gamma(2b+1)) \sinh(\lambda + i\gamma(2b-1))} \\ & \times (2 \sin^2 \gamma + \sinh^2 \lambda + \sinh^2(\lambda - i\gamma) + \sinh^2(\lambda - 2i\gamma b) + \\ & \sinh^2(\lambda - i\gamma(2b+1)) - \sinh^2[2\lambda - i\gamma(2b+1)]) . \end{aligned} \quad (\text{B4})$$

This state has  $S_3 = 0$ . For generic  $b \neq 0$  (B4) is not invariant under charge conjugation  $b \leftrightarrow -b$ , therefore the eigenvalue in the  $(N_1, N_2) = (0, 2)$  sector corresponding to the solution  $\lambda_1^{(2)} = 0$ ,  $\lambda_2^{(2)} = i\pi/2$  of the Bethe equations is

$$\Lambda_{02}^{(b,\{b,-b\})}(\lambda) = \Lambda_{20}^{(-b,\{b,-b\})}(\lambda). \quad (\text{B5})$$

- $(N_1, N_2) = (1, 1)$ :

In this sector we have three different eigenvalues corresponding to rather peculiar solutions of the Bethe equations:

The first solution is actually a one parametric family defined by

$$\cosh(\lambda^{(1)} + \lambda^{(2)}) \cos(\gamma) = \cosh(\lambda^{(1)} - \lambda^{(2)}) \cos(2\gamma b). \quad (\text{B6})$$

The eigenvalue corresponding to all solutions of (B6) is

$$\Lambda_{11,0}^{(b,\{b,-b\})}(\lambda) = - \left( \frac{\sin \gamma}{\sinh(\lambda - i\gamma)} \right)^2 \frac{\sin(\gamma(2b+1)) \sin(\gamma(2b-1))}{\sinh(\lambda - i\gamma(2b+1)) \sinh(\lambda + i\gamma(2b-1))}. \quad (\text{B7})$$

It appears twice in the spectrum of  $T^{(b)}(\lambda)$ .

Additional solutions to the Bethe equations in this sector involve at least one root at  $\pm\infty$ .

Choosing  $\lambda^{(1)} = -\infty$  the other Bethe equations becomes

$$\frac{\sinh(\lambda^{(2)} + i\gamma(b - \frac{1}{2}))}{\sinh(\lambda^{(2)} - i\gamma(b - \frac{1}{2}))} \frac{\sinh(\lambda^{(2)} - i\gamma(b + \frac{1}{2}))}{\sinh(\lambda^{(2)} + i\gamma(b + \frac{1}{2}))} = e^{-2i\gamma}. \quad (\text{B8})$$

This equation has two solutions: the first one is contained in (B6) leading to the eigenvalue (B7) discussed above, while for the other one  $\lambda^{(2)} = +\infty$  leading to the eigenvalue

$$\begin{aligned} \Lambda_{11,+}^{(b,\{b,-b\})}(\lambda) = & -\frac{1}{4} \left( \frac{\sin \gamma}{\sinh(\lambda - i\gamma)} \right)^2 \frac{1}{\sinh(\lambda - i\gamma(2b+1)) \sinh(\lambda + i\gamma(2b-1))} \\ & \times \left[ e^{2\lambda - i\gamma} (1 + e^{-4i\gamma b}) - 2 \cos \gamma \right] \left[ e^{-2\lambda + i\gamma} (1 + e^{-4i\gamma b}) - 2 \cos \gamma \right]. \end{aligned} \quad (\text{B9})$$

Although this eigenvalue is found in the zero charge sector of the model it is not invariant under charge conjugation  $b \leftarrow -b$ . In fact, choosing the solution  $\lambda^{(1)} = +\infty$  and  $\lambda^{(2)} = -\infty$  to the Bethe equations we obtain a third eigenvalue in this sector, i.e.

$$\Lambda_{11,-}^{(b,\{b,-b\})}(\lambda) = \Lambda_{11,+}^{(-b,\{b,-b\})}(\lambda). \quad (\text{B10})$$

Finally, let us remark on the limit  $b \rightarrow \pm\frac{1}{2}$ : in the rational  $sl(2|1)$ -invariant case the four dimensional 'typical' representation  $[b, \frac{1}{2}]$  degenerates into one of the three-dimensional atypical ones  $[\frac{1}{2}]_{\pm}$  [7]. Similarly, the decomposition of the tensor product of two such representations degenerates in the limit with  $b_1 = -b_2 \equiv b \rightarrow \pm\frac{1}{2}$ . Instead of the  $sl(2|1)$  octet  $[0, 1]$  and an eight-dimensional indecomposable one finds an octet and an  $sl(2|1)$  singlet:

$$\begin{aligned} \left[ b, \frac{1}{2} \right] \otimes \left[ -b, \frac{1}{2} \right] &= [0, 1] \oplus \left[ 0, \frac{1}{2}, -\frac{1}{2}, 0 \right] \\ \Rightarrow \left[ \frac{1}{2} \right]_+ \otimes \left[ \frac{1}{2} \right]_- &= [0, 1] \oplus [0]. \end{aligned} \quad (\text{B11})$$

Periodic boundary conditions break the symmetry of the  $q$ -deformed vertex model but still one observes degenerations arising in the limit  $b \rightarrow \pm\frac{1}{2}$ . This shows up through singularities in the vertex weights (A1) of the  $U_q[sl(2|1)]$  model. They allow to obtain a fusion relation from the Yang-Baxter equation for the monodromy matrix which can be exploited to construct integrable models with higher spin. Another consequence of these singularities is that part of the Hilbert space of the mixed vertex model decouples leaving the model built from the three-dimensional quark and antiquark representations [5, 17] as the non-trivial part.

For the two-site model considered here this leads to the vanishing of the eigenvalues (B2) and (B7) for any values of the deformation parameter  $\gamma$  while

$$\Lambda_{20}^{(\pm\frac{1}{2}, \{\frac{1}{2}, -\frac{1}{2}\})}(\lambda) = \Lambda_{02}^{(\pm\frac{1}{2}, \{\frac{1}{2}, -\frac{1}{2}\})}(\lambda) \equiv -4 \sin^2 \gamma \quad (\text{B12})$$

become independent of the spectral parameter  $\lambda$ . For the superspin chain Hamiltonian (2.11) this implies the appearance of zero energy eigenvalues. Eliminating the decoupled states from the Hilbert space only one of the singlets (B7) remains in the spectrum. This state, parameterized by Bethe roots  $\lambda^{(1)} = \lambda^{(2)} = 0$ , is  $c = 0$  ground state of the antiferromagnetic  $3 \otimes \bar{3}$ -superspin chain discussed in Refs. 5 and 17 for  $L = 1$ .

- 
- [1] I. Affleck, Nucl. Phys. B **265**, 409 (1986)
  - [2] I. Affleck and F. D. M. Haldane, Phys. Rev. B **36**, 5291 (1987)
  - [3] M. J. Martins, B. Nienhuis, and R. Rietman, Phys. Rev. Lett. **81**, 504 (1998), cond-mat/9709051
  - [4] H. Saleur, Nucl. Phys. B **578**, 552 (2000), solv-int/9905007
  - [5] F. H. L. Essler, H. Frahm, and H. Saleur, Nucl. Phys. B **712** [FS], 513 (2005), cond-mat/0501197
  - [6] Y. Ikhlef, J. L. Jacobsen, and H. Saleur, Nucl. Phys. B **789**, 483 (2008), cond-mat/0612037
  - [7] M. Scheunert, W. Nahm, and V. Rittenberg, J. Math. Phys. **18**, 155 (1977)
  - [8] A. J. Bracken, M. D. Gould, Y.-Z. Zhang, and G. W. Delius, J. Phys. A **27**, 6551 (1994), hep-th/9405138
  - [9] G. W. Delius, M. D. Gould, J. R. Links, and Y.-Z. Zhang, Int. J. Mod. Phys. A **10**, 3259 (1995), hep-th/9408006
  - [10] Z. Maassarani, J. Phys. A **28**, 1305 (1995), hep-th/9407032
  - [11] J. Gruneberg, Nuclear Physics B **568**, 594 (2000)
  - [12] P. P. Kulish, J. Sov. Math. **35**, 2648 (1986), [Zap. Nauch. Semin. LOMI **145**, 140 (1985)]
  - [13] M. P. Pfannmüller and H. Frahm, Nucl. Phys. B **479**, 575 (1996), cond-mat/9604082
  - [14] M. P. Pfannmüller and H. Frahm, J. Phys. A **30**, L543 (1997)
  - [15] P. B. Ramos and M. J. Martins, Nucl. Phys. B **474** [FS], 678 (1996), hep-th/9604072
  - [16] W. Galleas and M. J. Martins, Nucl. Phys. B **768**, 219 (2007), hep-th/0612281
  - [17] H. Frahm and M. J. Martins, Nucl. Phys. B **847**, 220 (2011), arXiv:1012.1753
  - [18] H. N. V. Temperley and E. H. Lieb, Proc. R. Soc. Lond. A **332**, 251 (1971)
  - [19] R. J. Baxter, S. B. Kelland, and F. Y. Wu, J. Phys. A **9**, 397 (1976)
  - [20] R. J. Baxter, Proc. R. Soc. Lond. A **383**, 43 (1982)
  - [21] L. A. Takhtajan and L. D. Faddeev, Russ. Math. Survey **34**, 11 (1979)
  - [22] V. E. Korepin, N. M. Bogoliubov, and A. G. Izergin, *Quantum Inverse Scattering Method and Correlation Functions* (Cambridge University Press, Cambridge, 1993)
  - [23] A. B. Zamolodchikov and V. A. Fateev, Sov. J. Nucl. Phys. **32**, 298 (1980)
  - [24] M. Jimbo, Comm. Math. Phys. **102**, 537 (1986)
  - [25] M. J. Martins, Phys. Rev. E **59**, 7220 (1999)
  - [26] U. Grimm, J. Phys. A **27**, 5897 (1994)
  - [27] W. Galleas and M. J. Martins, Nucl. Phys. B **732**, 444 (2006), nlin/0509014
  - [28] Y. Ikhlef, J. L. Jacobsen, and H. Saleur, J. Phys. A **43**, 225201 (2010), arXiv:0911.3003
  - [29] M. Takahashi and M. Suzuki, Prog. Theor. Phys. **48**, 2187 (1972)
  - [30] C. N. Yang and C. P. Yang, J. Math. Phys. **10**, 1115 (1969)
  - [31] F. H. L. Essler, H. Frahm, F. Göhmann, A. Klümper, and V. E. Korepin, *The One-Dimensional Hubbard Model* (Cambridge University Press, Cambridge (UK), 2005)
  - [32] H. J. de Vega and F. Woynarowich, Nucl. Phys. B **251**, 439 (1985)



- [33] H. J. de Vega, J. Phys. A: Math. Gen. **21**, L1089 (1988)
- [34] F. Woynarovich and H.-P. Eckle, J. Phys. A **20**, L443 (1987)
- [35] J. Suzuki, J. Phys. A: Math. Gen. **21**, L1175 (1988)
- [36] H. W. J. Blöte, J. L. Cardy, and M. P. Nightingale, Phys. Rev. Lett. **56**, 742 (1986).
- [37] I. Affleck, Phys. Rev. Lett. **56**, 746 (1986).
- [38] N. Yu and M. Fowler, Phys. Rev. B **46**, 14583 (1992)
- [39] J. L. Jacobsen and H. Saleur, Nucl. Phys. B **743**, 207 (2006), cond-mat/0512058
- [40] J. L. Cardy, Nucl. Phys. B **270**, 186 (1986)
- [41] Y. Ikhlef, Mod. Phys. Lett. B **25**, 291 (2011), arXiv:1012.2380
- [42] V. Y. Popkov and A. A. Zvyagin, Phys. Lett. A **175**, 295 (1993)
- [43] H. Frahm and C. Rödenbeck, J. Phys. A **30**, 4467 (1997), cond-mat/9702083
- [44] C. J. Hamer, J. Phys. A **18**, L1133 (1985)
- [45] F. Woynarovich and H.-P. Eckle, J. Phys. A **20**, L97 (1987)
- [46] F. C. Alcaraz, M. N. Barber, and M. T. Batchelor, Phys. Rev. Lett. **58**, 771 (1987)
- [47] H. Frahm, M. P. Pfannmüller, and A. M. Tsvelik, Phys. Rev. Lett. **81**, 2116 (1998), cond-mat/9803145
- [48] H. Frahm, Nucl. Phys. B **559**, 613 (1999), cond-mat/9904157
- [49] F. C. Alcaraz and M. J. Martins, Phys. Rev. Lett. **63**, 708 (1989)
- [50] F. C. Alcaraz and M. J. Martins, J. Phys. A **22**, 1829 (1989)
- [51] H. Frahm, N.-C. Yu, and M. Fowler, Nucl. Phys. B **336**, 396 (1990)
- [52] H. Frahm and N.-C. Yu, J. Phys. A **23**, 2115 (1990)

TABLE I. Finite-size sequences (4.15) of the anomalous dimension  $X_{1,0}^{0,0}(\gamma)$  corresponding to the ground state of the antiferromagnetic mixed superspin chain for  $\gamma = 2\pi/5, 2\pi/9$  and  $b = 0.1, 0.2, 0.3, 0.4$  from the Bethe ansatz. The expected exact conformal dimension is  $X_{1,0}^{0,0}(\gamma) = \frac{1}{4}$ , independent of  $\gamma$  and  $b$ .

$X_{1,0}^{0,0}(2\pi/5)$	$b = 0.1$	$b = 0.2$	$b = 0.3$	$b = 0.4$
64	0.250048612966262	0.250057352809966	0.250079908701413	0.250153486545075
68	0.250044800002668	0.250052960280743	0.250074088242237	0.250143781486991
72	0.250041480552865	0.250049125512265	0.250068974707988	0.250135085547961
76	0.250038568285938	0.250045752223167	0.250064450636514	0.250127260002517
80	0.250035995187684	0.250042765513805	0.250060424128183	0.250120188361586
84	0.250033708784690	0.250040103975741	0.250056819907415	0.250113771814941
88	0.250031664084155	0.250037719523553	0.250053577683175	0.250107929518090
92	0.250029826347013	0.250035574034939	0.250050646736442	0.250102591235422
96	0.250028167338885	0.250033632461034	0.250047987323579	0.250097698864218
100	0.250026663737575	0.250031869300816	0.250045563476697	0.250093198867507
Extrap.	0.250002(1)	0.250001(1)	0.24999984(2)	0.2500001(3)
$X_{1,0}^{0,0}(2\pi/9)$	$b = 0.1$	$b = 0.2$	$b = 0.3$	$b = 0.4$
64	0.253132058479334	0.253431444329609	0.254106625377260	0.255863205280181
68	0.253025177990501	0.253314682476050	0.253967922029803	0.255670948431118
72	0.252927764888214	0.253208226471161	0.253841349125435	0.255494860072799
76	0.252838520004755	0.253110668379048	0.253725265274230	0.255332854789668
80	0.252756378517378	0.253020852585427	0.253618322313239	0.255183198042987
84	0.252680460193235	0.252937821882064	0.253519399812617	0.255044436405680
88	0.252610028646216	0.252860776548557	0.253427560977248	0.254915339947881
92	0.252544463265816	0.252789041850631	0.253342011784391	0.254794862710576
96	0.252483237655954	0.252722043984628	0.253262079561925	0.254682108820548
100	0.252425899534380	0.252659291643748	0.253187183973606	0.254576304302893
Extrap.	0.25003(2)	0.24995(3)	0.25004(2)	0.24997(2)

TABLE II. Finite-size sequences (4.15) of the anomalous dimension  $X_{0,0}^{\frac{1}{2},\frac{1}{2}}(\gamma)$  of the antiferromagnetic mixed superspin chain for  $\gamma = 2\pi/5, 2\pi/9$  and  $b = 0.1, 0.2, 0.3, 0.4$  from the Bethe ansatz. The expected exact conformal dimensions are  $X_{0,0}^{\frac{1}{2},\frac{1}{2}}(2\pi/5) = 5/12$  and  $X_{0,0}^{\frac{1}{2},\frac{1}{2}}(2\pi/9) = 9/28$  independent of  $b$ .

$X_{0,0}^{\frac{1}{2},\frac{1}{2}}(2\pi/5)$	$b = 0.1$	$b = 0.2$	$b = 0.3$	$b = 0.4$
64	0.416670417631978	0.416656218465817	0.416610197227320	0.416354881252023
68	0.416669987565812	0.416657408090032	0.416616640599484	0.416390524909717
72	0.416669627133090	0.416658405958250	0.416622040898389	0.416420383057850
76	0.416669322128664	0.416659250096786	0.416626611560886	0.41644564432787
80	0.416669062413019	0.416659971230323	0.416630513869716	0.416467205721020
84	0.416668838812804	0.416660591916285	0.416633872109781	0.416485757527825
88	0.416668644721943	0.416661070729271	0.416636783046771	0.416501777174014
92	0.416668475963537	0.416661547020412	0.416639322642474	0.416515806307798
96	0.416668327514699	0.416661965760863	0.416641552261224	0.416528116518884
100	0.416668196783305	0.416662334075060	0.416643519898230	0.416538978974116
Extrap.	0.416667(1)	0.4166663(1)	0.416667(2)	0.416667(3)
$X_{0,0}^{\frac{1}{2},\frac{1}{2}}(2\pi/9)$	$b = 0.1$	$b = 0.2$	$b = 0.3$	$b = 0.4$
64	0.321478885785230	0.321480244434995	0.321478675589893	0.321419894207957
68	0.321475362972286	0.321477017780511	0.321476806551588	0.321428958054849
72	0.321472274265546	0.321474149284625	0.321475003385914	0.321436049810230
76	0.321469545411844	0.321471583890475	0.321473278305405	0.321441630433088
80	0.321467123806211	0.321469276575399	0.321471637081771	0.321446038562155
84	0.321464951878455	0.321467191544666	0.321470080991823	0.321449528944129
88	0.321462997920481	0.321465298207456	0.321468607979076	0.321452293350554
92	0.321461231497336	0.321463572029351	0.321467215870929	0.321454479967015
96	0.321459626953652	0.321461991599086	0.321465900513161	0.321456201956970
100	0.321458164206755	0.321460540439523	0.321464653145202	0.321457549599824
Extrap.	0.321458(1)	0.321426(3)	0.321426(1)	0.32143(1)

TABLE III. Finite-size sequences (4.15) of the anomalous dimension  $X_{1,-1}^{\frac{1}{2},\frac{1}{2}}(\gamma)$  of the antiferromagnetic mixed superspin chain for  $\gamma = 2\pi/5, 2\pi/9$  and  $b = 0.1, 0.2, 0.3, 0.4$  from the Bethe ansatz. The expected exact conformal dimensions are  $X_{1,-1}^{\frac{1}{2},\frac{1}{2}}(2\pi/5) = 49/60$  and  $X_{1,-1}^{\frac{1}{2},\frac{1}{2}}(2\pi/9) = 137/252$  independent of  $b$ .

$X_{1,-1}^{\frac{1}{2},\frac{1}{2}}(2\pi/5)$	$b = 0.1$	$b = 0.2$	$b = 0.3$	$b = 0.4$
64	0.802543420915095	0.800996714941326	0.797451714287750	0.788002733672379
68	0.803109142135808	0.801619792314736	0.798202751578452	0.789061829077160
72	0.803621371338520	0.802184427361242	0.798884681127158	0.790029738004235
76	0.804087771606711	0.802698923084324	0.799507125805111	0.790918241220402
80	0.804514571755953	0.803170041748389	0.800077960470532	0.791737149187162
84	0.804906894958283	0.803603354252052	0.800603695001582	0.792494698387001
88	0.805268993033042	0.804003490361879	0.801089763004215	0.793197855830765
92	0.805604428993397	0.804374337112643	0.801540740173121	0.793852555009990
96	0.805916212570146	0.804719178147089	0.801960503234090	0.794463882917438
100	0.806206904992800	0.805040815482502	0.802352368121435	0.79503622240196
Extrap.	0.81661(2)	0.81667(1)	0.8166(2)	0.8174(2)
$X_{1,-1}^{\frac{1}{2},\frac{1}{2}}(2\pi/9)$	$b = 0.1$	$b = 0.2$	$b = 0.3$	$b = 0.4$
64	0.469649001673299	0.466575740909034	0.460184330193937	0.445977608618501
68	0.470774831559801	0.467741761599685	0.461432012191324	0.447396493043942
72	0.471822545482396	0.468827088511210	0.462593839845175	0.448719147269481
76	0.472801422875943	0.469841288401414	0.463679948377037	0.449956804126546
80	0.473719226661201	0.470792368025533	0.464698825642782	0.451118889793702
84	0.474582512357382	0.471687089632269	0.465657646470560	0.452213383888303
88	0.475396863517694	0.472531215460570	0.466562525609641	0.453247098947592
92	0.476167071653444	0.473329690796934	0.467418715541751	0.454225894135166
96	0.476897277726334	0.474086790324252	0.468230758833534	0.455154844481359
100	0.477591081020453	0.474806231909338	0.469002608145475	0.456038369643072
Extrap.	0.5469(2)	0.546(1)	0.5492(2)	0.547(1)

TABLE IV. Finite-size sequences (4.15) of the anomalous dimension  $X_{1,0}^{1,0}(\gamma)$  of the antiferromagnetic mixed superspin chain for  $\gamma = 2\pi/5, 2\pi/9$  and  $b = 0.1, 0.2, 0.3, 0.4$  from the Bethe ansatz. The expected exact conformal dimensions are  $X_{1,0}^{1,0}(2\pi/5) = 31/24$  and  $X_{1,0}^{1,0}(2\pi/9) = 95/56$  independent of  $b$ .

$X_{1,0}^{1,0}(2\pi/5)$	$b = 0.1$	$b = 0.2$	$b = 0.3$	$b = 0.4$
64	1.29169391271122	1.29188030171550	1.29246176734499	1.29549189382126
68	1.29169747618030	1.29186417985947	1.29238361004235	1.29508481229779
72	1.29169998846533	1.29185008220992	1.29231721713292	1.29474153535161
76	1.29170171985766	1.29183766315244	1.29226028317640	1.29444925164532
80	1.29170286782319	1.29182665069729	1.29221104956300	1.29419822711471
84	1.29170357644233	1.29181682617240	1.29216815127140	1.29398095434414
88	1.29170395121063	1.29180801570822	1.29213051785738	1.29379156808294
92	1.29170407360045	1.29180007506879	1.29209729685151	1.29362543257076
96	1.29170400266840	1.29179288604481	1.29206780649186	1.29347884081817
100	1.29170378640977	1.29178635018844	1.29204149259774	1.29334880116668
Extrap.	1.2917(1)	1.29165(2)	1.291665(2)	1.291667(1)
$X_{1,0}^{1,0}(2\pi/9)$	$b = 0.1$	$b = 0.2$	$b = 0.3$	$b = 0.4$
64	1.65831148570030	1.65491024458575	1.64745726183318	1.63027640189379
68	1.65967750746320	1.65637015514941	1.64909748064187	1.63208407458946
72	1.66091746837352	1.65769829971046	1.65059835126374	1.63378198262557
76	1.66204931417987	1.65891300418380	1.65197797284606	1.63537771386844
80	1.66308763279172	1.66002924590730	1.65325137518418	1.63687886760066
84	1.66404441718139	1.66105939574434	1.65443114647623	1.63829274704172
88	1.66492962800063	1.66201377134831	1.65552791636658	1.63962620939402
92	1.66575161458998	1.66290105323150	1.65655072391135	1.64088560250871
96	1.66651743360543	1.66372860292841	1.65750730871397	1.64207675144390
100	1.66723309416254	1.66450270787275	1.65840433835020	1.64320497592494
Extrap.	1.69638(2)	1.69638(1)	1.6969(3)	1.661(3)

TABLE V. Finite-size sequences (4.15) of the anomalous dimension  $X_{1,1}^{\frac{1}{2},\frac{1}{2}}(\gamma)$  of the antiferromagnetic mixed superspin chain for  $\gamma = 2\pi/5, 2\pi/9$  and  $b = 0.1, 0.2, 0.3, 0.4$  from the Bethe ansatz. The expected exact conformal dimensions are  $X_{1,1}^{\frac{1}{2},\frac{1}{2}}(2\pi/5) = 61/60$  and  $X_{1,1}^{\frac{1}{2},\frac{1}{2}}(2\pi/9) = 277/252$  independent of  $b$ .

$X_{1,1}^{\frac{1}{2},\frac{1}{2}}(2\pi/5)$	$b = 0.1$	$b = 0.2$	$b = 0.3$	$b = 0.4$
64	1.01660809460145	1.01674796672621	1.01720030948687	1.01970307551162
68	1.01661480621747	1.01673872337252	1.01713948238592	1.01935718467132
72	1.01662042714845	1.01673097085398	1.01708849236842	1.01906718883947
76	1.01662518207921	1.01672440643128	1.01704532699284	1.01882166496922
80	1.01662923940361	1.01671879759808	1.01700846418273	1.01861196515601
84	1.01663273029972	1.01671396921624	1.01697673295315	1.01843144543536
88	1.01663575356290	1.01670978164280	1.01694922441500	1.01827493321853
92	1.01663839163587	1.01670612582146	1.01692522084310	1.01813835363556
96	1.01664070491891	1.01670291651396	1.01690415103221	1.01801845973993
100	1.01664274594897	1.01670008430629	1.01688555504759	1.01791264141798
Extrap.	1.01665(1)	1.01665(2)	1.016663(1)	1.06665(3)
$X_{1,1}^{\frac{1}{2},\frac{1}{2}}(2\pi/9)$	$b = 0.1$	$b = 0.2$	$b = 0.3$	$b = 0.4$
64	1.09896258489785	1.09906445762706	1.09941621118507	1.10154807320311
68	1.09898211749043	1.09907068232367	1.09937791947098	1.10125137082147
72	1.09899899574197	1.09907651035724	1.09934670412561	1.10100445331082
76	1.09901370764206	1.09908195585909	1.09932102076494	1.10079694624626
80	1.09902663078237	1.09908704065466	1.09929971588858	1.10062102508163
84	1.09903806201443	1.09909178836045	1.09928191439564	1.10047070214516
88	1.09904823720116	1.09909622419276	1.09926694360684	1.10034133469567
92	1.09905734493280	1.09910037169640	1.09925428104614	1.10022927695166
96	1.09906553989567	1.09910425310586	1.09924351573734	1.10013163872575
100	1.09907294839689	1.09910789126798	1.09923432056007	1.10004610173584
Extrap.	1.09922(1)	1.09921(2)	1.0991(1)	1.0991(2)

TABLE VI. Finite-size sequences (4.15) of the anomalous dimension  $X_{1,0}^{1,1}(\gamma)$  of the antiferromagnetic mixed superspin chain for  $\gamma = 2\pi/5, 2\pi/9$  and  $b = 0.1, 0.2, 0.3, 0.4$  from the Bethe ansatz. The expected exact conformal dimensions are  $X_{1,0}^{1,1}(2\pi/5) = 23/12$  and  $X_{1,0}^{1,1}(2\pi/9) = 43/28$  independent of  $b$ .

$X_{1,0}^{1,1}(2\pi/5)$	0.1	0.2	0.3	0.4
64	1.91633350061679	1.91671340547377	1.91794265757312	1.92474331627926
68	1.91637144225241	1.91670796028526	1.91779690210299	1.92382383023129
72	1.91640325233943	1.91670340851577	1.91767474571176	1.92305262480562
76	1.91643018323036	1.91669956611603	1.91757135907367	1.92239949136765
80	1.91645318416930	1.91669629383031	1.91748308691517	1.92184153275738
84	1.91647298557160	1.91669348333802	1.91740712239614	1.92136113809079
88	1.91649015396588	1.91669105320029	1.91734128093283	1.9209445839460
92	1.91650513545003	1.91668893792311	1.91728384016498	1.92058105193391
96	1.91651828702507	1.91668708483102	1.91723343201604	1.92026191802231
100	1.91652989610853	1.91668545343676	1.91718895267849	1.91998024230886
Extrap.	1.91666(1)	1.91665(1)	1.91666(2)	1.9166(1)
$X_{1,0}^{1,1}(2\pi/9)$	0.1	0.2	0.3	0.4
64	1.54595893269632	1.54714023224294	1.55001371490657	1.55969299725040
68	1.54564437619687	1.54677034969013	1.54949371360320	1.55852248544641
72	1.54535487074355	1.54643219432769	1.54902475966904	1.55749654171679
76	1.54508734785315	1.54612150411845	1.54859900060520	1.55658895839048
80	1.54483923019746	1.54583477645593	1.54821017751172	1.55577950742735
84	1.54460833610583	1.54556910385993	1.54785323101280	1.55505233513379
88	1.54439280622750	1.54532204968426	1.54752402474063	1.55439485052312
92	1.54419104585411	1.54509155364219	1.54721913528093	1.55379692588342
96	1.54400168081111	1.54487586080783	1.54693570616330	1.55325032866461
100	1.54382351731674	1.54467346577192	1.54667132942653	1.55274829423512
Extrap.	1.5356(1)	1.5358(1)	1.5351(2)	1.535(1)

TABLE VII. Finite-size sequences (4.25) of the anomalous dimension  $X_{1,0}^{0,0}(\gamma)$  corresponding to the ground state of the ferromagnetic mixed superspin chain for  $\gamma = 2\pi/5, 2\pi/9$  and  $b = 0.1, 0.2, 0.3, 0.4$  from the Bethe ansatz. The expected exact conformal dimension is  $X_{1,0}^{0,0}(\gamma) = \frac{1}{4}$  independent of  $\gamma$  and  $b$ .

$X_{1,0}^{0,0}(2\pi/5)$	$b = 0.1$	$b = 0.2$	$b = 0.3$	$b = 0.4$
4	0.249618388905792	0.249864078062197	0.250380674609993	0.251433496876099
8	0.249912388797508	0.249965813355377	0.250079922137901	0.250320222469547
12	0.249962057861862	0.249985305677197	0.250035162436907	0.250140964674203
16	0.249978921372708	0.249991918899564	0.250019836847325	0.250079269513615
20	0.249986607712271	0.249994907534576	0.250012748900962	0.250050790847099
24	0.249990744279497	0.249996502689051	0.250008886931439	0.250035317308795
28	0.249993222825207	0.249997451946100	0.250006549862109	0.250025978300525
32	0.249994824338185	0.249998061879352	0.250005028056580	0.250019910102813
36	0.249995918536672	0.249998476736720	0.250003981517046	0.250015745271696
40	0.249996699224027	0.249998771167758	0.250003231052877	0.250012763515263
Extrap.	0.25000003(2)	0.25000005(1)	0.25000007(2)	0.2499996(3)
$X_{1,0}^{0,0}(2\pi/9)$	$b = 0.1$	$b = 0.2$	$b = 0.3$	$b = 0.4$
4	0.244044806842760	0.244461720024188	0.245172840974522	0.246203546383614
8	0.248700725305516	0.248802997575032	0.248979563899314	0.249240366426739
12	0.249434549177625	0.249479482670048	0.249557418184965	0.249673343839989
16	0.249684085421290	0.249709260050335	0.249752996660027	0.249818218822082
20	0.249798433771513	0.249814515658493	0.249842476615247	0.249884223298235
24	0.249860253886827	0.249871410635206	0.249890816324928	0.249919808908815
28	0.249897430776020	0.249905622406331	0.249919874671653	0.249941175992748
32	0.249921520599999	0.249927789931196	0.249938699258291	0.249955008463470
36	0.249938018641971	0.249942970904318	0.249951589132296	0.249964475692600
40	0.249949810553310	0.249953821065760	0.249960801110223	0.249971239248729
Extrap.	0.25000003(2)	0.25000007(3)	0.25000002(2)	0.250000031(1)



TABLE VIII. Finite-size sequences (4.25) of the anomalous dimension  $X_{0,0}^{\frac{1}{2},-\frac{1}{2}}(\gamma)$  of the ferromagnetic mixed superspin chain for  $\gamma = 2\pi/5, 2\pi/9$  and  $b = 0.1, 0.2, 0.3, 0.4$  from the Bethe ansatz. The expected exact conformal dimensions are  $X_{0,0}^{\frac{1}{2},-\frac{1}{2}}(2\pi/5) = 5/12$  and  $X_{0,0}^{\frac{1}{2},-\frac{1}{2}}(2\pi/9) = 9/28$  independent of  $b$ .

$X_{0,0}^{\frac{1}{2},-\frac{1}{2}}(2\pi/5)$	$b = 0.1$	$b = 0.2$	$b = 0.3$	$b = 0.4$
4	0.420153202195165	0.418311223187811	0.414094943222730	0.40447340188129
8	0.417533635282876	0.417139647726513	0.416282739919060	0.414402513758005
12	0.417050902689717	0.416880022540026	0.416510598502611	0.415713015644990
16	0.416882479860486	0.416787136134762	0.416581379806527	0.416139003433824
20	0.416804662357638	0.416743862247532	0.416612753609402	0.416331359972793
24	0.416762438843948	0.416720296295040	0.416629457157763	0.416434667265353
28	0.416736999096700	0.416706071365318	0.416639421617616	0.416496576350315
32	0.416720497319091	0.416696834653756	0.416645848671003	0.416536610323140
36	0.416709188622272	0.416690500639723	0.416650237899716	0.416563993281584
40	0.416701102495937	0.416685969815732	0.416653369568434	0.416583549056764
Extrap.	0.41666668(2)	0.41666662(3)	0.4166665(3)	0.4166661(3)
$X_{0,0}^{\frac{1}{2},-\frac{1}{2}}(2\pi/9)$	$b = 0.1$	$b = 0.2$	$b = 0.3$	$b = 0.4$
4	0.319913713673340	0.320018967155828	0.320190591772206	0.320420310281376
8	0.321157712483394	0.321191122084441	0.321248225946738	0.321331244861727
12	0.321314654780622	0.321329741251375	0.321355797251027	0.321394295060097
16	0.321365627553391	0.321374157960506	0.321388943280466	0.321410910201736
20	0.321388611392069	0.321394083529534	0.321403583460742	0.321417733723489
24	0.321400941690716	0.321404746407637	0.321411357486342	0.321421218332086
28	0.321408324757022	0.321411122201603	0.321415985350110	0.321423245212332
32	0.321413096052956	0.321415238901914	0.321418965356214	0.321424531307902
36	0.321416358100397	0.321418051745520	0.321420997553802	0.321425399388384
40	0.321418686741470	0.321420059101585	0.321422446146568	0.321426013997661
Extrap.	0.321425(2)	0.321428(34)	0.3214285(3)	0.3214286(3)

TABLE IX. Finite-size sequences (4.25) of the anomalous dimension  $X_{1,1}^{\frac{1}{2},-\frac{1}{2}}(\gamma)$  of the ferromagnetic mixed superspin chain for  $\gamma = 2\pi/5, 2\pi/9$  and  $b = 0.1, 0.2, 0.3, 0.4$  from the Bethe ansatz. The expected exact conformal dimensions are  $X_{1,1}^{\frac{1}{2},-\frac{1}{2}}(2\pi/5) = 49/60$  and  $X_{1,1}^{\frac{1}{2},-\frac{1}{2}}(2\pi/9) = 137/252$  independent of  $b$ .

$X_{1,1}^{\frac{1}{2},-\frac{1}{2}}(2\pi/5)$	$b = 0.1$	$b = 0.2$	$b = 0.3$	$b = 0.4$
4	0.804938854579059	0.814319917467641	0.834792393417294	0.879143521859337
8	0.813596692907556	0.815893063874643	0.820852468461199	0.831532156138152
12	0.815277718645391	0.816292762124510	0.818482319585240	0.823183312552782
16	0.815878039474781	0.816447384142183	0.817674984015266	0.820308238730800
20	0.816159032430526	0.816522772350630	0.817306868984783	0.818988000334640
24	0.816312767449947	0.816565061146465	0.817108836773558	0.818274369988834
28	0.816405927448350	0.816591124286526	0.816990242152023	0.817845542170740
32	0.816466614117071	0.816608311410614	0.816913659290931	0.817567916228810
36	0.816508337929270	0.816620237845708	0.816861360234222	0.817377944643833
40	0.816538249251599	0.816628850050168	0.816824067600668	0.817242267787161
Extrap.	0.81666693(2)	0.8166668(2)	0.8166675(2)	0.816673(2)
$X_{1,1}^{\frac{1}{2},-\frac{1}{2}}(2\pi/9)$	$b = 0.1$	$b = 0.2$	$b = 0.3$	$b = 0.4$
4	0.533880505305017	0.534967698841839	0.536853524001006	0.539660072909485
8	0.541383434410729	0.541648424113656	0.542108818742814	0.542795515425274
12	0.542654427057378	0.542771434479493	0.542974956206111	0.543279030322532
16	0.543092408233721	0.543158077439541	0.543272348894322	0.543443184803063
20	0.543294026061150	0.543336010860762	0.543409082836059	0.543518357900393
24	0.543403261934016	0.543432401612150	0.543483122740523	0.543558985879656
28	0.543469032017435	0.543490433589493	0.543527687861490	0.543583414067994
32	0.543511681223300	0.543528063059823	0.543556580857472	0.543599241290840
36	0.543540903977126	0.543553845883840	0.543576375481245	0.543610079844243
40	0.543561798440967	0.543572279952902	0.543590527601463	0.543617826543895
Extrap.	0.543652(2)	0.0543653(1)	0.5436508(2)	0.5436508(3)

TABLE X. Finite-size sequences (4.25) of the anomalous dimension  $X_{1,1}^{\frac{1}{2},\frac{1}{2}}(\gamma)$  of the ferromagnetic mixed superspin chain for  $\gamma = 2\pi/5, 2\pi/9$  and  $b = 0.1, 0.2, 0.3, 0.4$  from the Bethe ansatz. The expected exact conformal dimensions are  $X_{1,1}^{\frac{1}{2},\frac{1}{2}}(2\pi/5) = 41/40$  and  $X_{1,1}^{\frac{1}{2},\frac{1}{2}}(2\pi/9) = 97/72$  independent of  $b$ .

$X_{1,1}^{\frac{1}{2},\frac{1}{2}}(2\pi/5)$	$b = 0.1$	$b = 0.2$	$b = 0.3$	$b = 0.4$
4	0.994997978852449	1.00876393795618	1.03824887162911	1.10011863417448
8	1.01750044752832	1.02109273301685	1.02880785279794	1.04523038678615
12	1.02166727960952	1.02327839396988	1.02674367461960	1.03414003184710
16	1.02312543799154	1.02403462682038	1.02599129860889	1.03017264439620
20	1.02380030916302	1.02438306807198	1.02563757651283	1.02831998897873
24	1.02416689237986	1.02457191882455	1.02544395528163	1.02730916557915
28	1.02438792592022	1.02468564407009	1.02532670183939	1.02669814116381
32	1.02453138316540	1.02475939722319	1.02525039524152	1.02630094270188
36	1.02462973613628	1.02480993532828	1.02519798652844	1.02602834133088
40	1.02470008713720	1.02484607136855	1.02516045226876	1.02583320955474
Extrap.	1.0250002(2)	1.0250001(1)	1.0249997(3)	1.0249994(2)
$X_{1,1}^{\frac{1}{2},\frac{1}{2}}(2\pi/9)$	$b = 0.1$	$b = 0.2$	$b = 0.3$	$b = 0.4$
4	1.29876758647094	1.30325656988360	1.31102766447121	1.32254599554157
8	1.33452774930199	1.33573236225976	1.33782984630232	1.34096834546194
12	1.34154352562186	1.34208650591172	1.34303195767985	1.34444680084643
16	1.34402121289879	1.34432814492269	1.34486256347996	1.34566227355483
20	1.34517162315680	1.34536850730852	1.34571130659309	1.34622425907196
24	1.34579746591406	1.34593436028266	1.34617270652002	1.34652935177740
28	1.34617514127825	1.34627579182547	1.34645103251638	1.34671324708849
32	1.34642039180554	1.34649748974364	1.34663172250430	1.34683257472766
36	1.34658859119652	1.34664952840261	1.34675562343607	1.34691437258345
40	1.34670893138310	1.34675830227098	1.34684425932718	1.34697287559906
Extrap.	1.3472222(1)	1.3472222(2)	1.3472223(2)	1.3742224(3)

TABLE XI. Finite-size sequences (4.25) of the anomalous dimension  $X_{1,0}^{1,-1}(\gamma)$  of the ferromagnetic mixed superspin chain for  $\gamma = 2\pi/5, 2\pi/9$  and  $b = 0.1, 0.2, 0.3, 0.4$  from the Bethe ansatz. The expected exact conformal dimensions are  $X_{1,0}^{1,-1}(2\pi/5) = 23/12$  and  $X_{1,0}^{1,-1}(2\pi/9) = 43/28$  independent of  $b$ .

$X_{1,0}^{1,-1}(2\pi/5)$	$b = 0.1$	$b = 0.2$	$b = 0.3$	$b = 0.4$
4	1.92275836268774	1.93708511027515	1.96438958339881	2.00429835568618
8	1.91908565206600	1.92092744160645	1.92450401713200	1.93029738987036
12	1.91781098647046	1.91846609255480	1.91979319308352	1.92224186047280
16	1.91732324822074	1.91765863919210	1.91835375244184	1.91971517305235
20	1.91709049473449	1.91729520769754	1.91772483742181	1.91859227129214
24	1.91696227916640	1.91710065979594	1.91739323998151	1.91799427030424
28	1.91688438802683	1.91698436898660	1.91719675456519	1.91763773565356
32	1.91683360960376	1.91690931467571	1.91707063708865	1.91740796311456
36	1.91679869850490	1.91685805584467	1.91698481982676	1.91725118033239
40	1.91677368043983	1.91682149275017	1.91692376310090	1.91713941274508
Extrap.	1.9166665(3)	1.9166664(2)	1.9166667(4)	1.9166667(2)
$X_{1,0}^{1,-1}(2\pi/9)$	$b = 0.1$	$b = 0.2$	$b = 0.3$	$b = 0.4$
4	1.89267410304585	1.87067227593596	1.82808451415017	1.75087323907445
8	1.64192241218324	1.63438221960052	1.62092224163197	1.59994006363493
12	1.58476516588047	1.58126414904826	1.57510198900755	1.56571877644079
16	1.56369613535041	1.56169796597256	1.55819786351628	1.55290966874609
20	1.55374177481035	1.55245446377004	1.55020450327766	1.54681712875058
24	1.54827895082732	1.54738179557628	1.54581561424246	1.54346217373252
28	1.54496582300292	1.54430527807228	1.54315297687471	1.54142343412900
32	1.54280766022497	1.54230123042885	1.54141818784558	1.54009376604051
36	1.54132445289797	1.54092393191263	1.54022577993160	1.53917919299817
40	1.54026173042878	1.53993708895457	1.53937133167230	1.53852352062602
Extrap.	1.53571(1)	1.53573(2)	1.53571(2)	1.53572(2)

TABLE XII. Finite-size sequences (4.25) of the anomalous dimension  $X_{0,0}^{\frac{1}{2},\frac{1}{2}}(\gamma)$  of the ferromagnetic mixed superspin chain for  $\gamma = 2\pi/5, 2\pi/9$  and  $b = 0.1, 0.2, 0.3, 0.4$  from the Bethe ansatz. The expected exact conformal dimensions are  $X_{0,0}^{\frac{1}{2},\frac{1}{2}}(2\pi/5) = 5/8$  and  $X_{0,0}^{\frac{1}{2},\frac{1}{2}}(2\pi/9) = 9/8$  independent of  $b$ .

$X_{0,0}^{\frac{1}{2},\frac{1}{2}}(2\pi/5)$	0.1	0.2	0.3	0.4
4	0.630213720410703	0.628167445380927	0.623556940842337	0.613210392494294
8	0.626298472836777	0.625855321761323	0.624894142565653	0.622799370606034
12	0.625576535867603	0.625384174503429	0.624968726489793	0.624073859686108
16	0.625324185193522	0.625216855887439	0.624985345732743	0.624488157113924
20	0.625207443504917	0.625139008388433	0.624991474730969	0.624675026917663
24	0.625144044650655	0.625096616112297	0.624994398748262	0.624775292259350
28	0.625105822737553	0.625071019767160	0.624996025401022	0.624835333745489
32	0.625081017557765	0.625054392599770	0.624997026550134	0.624874137620650
36	0.625064012291477	0.625042986503641	0.624997688262107	0.624900666695744
40	0.625051849144170	0.625034824633739	0.624998149205000	0.624919605647811
Extrap.	0.62499996(1)	0.6250002(2)	0.624997(1)	0.62499995(1)
$X_{0,0}^{\frac{1}{2},\frac{1}{2}}(2\pi/9)$	0.1	0.2	0.3	0.4
4	1.14652880714786	1.14785606161029	1.15022589201266	1.15391189127984
8	1.12985951474016	1.13011226978579	1.13055659229965	1.13123131520870
12	1.12712669630877	1.12723438773761	1.12742271780656	1.12770646795383
16	1.12619019285676	1.12624989511655	1.12635410217068	1.12651064369857
20	1.12575996440568	1.12579791958604	1.12586410849908	1.12596339789932
24	1.12552709642448	1.12555335909051	1.12559913518060	1.12566775024573
28	1.12538696538072	1.12540621828467	1.12543976663790	1.12549002936557
32	1.12529612700170	1.12531084678639	1.12533649097860	1.12537489994630
36	1.12523389945651	1.12524551879330	1.12526575843882	1.12529606621631
40	1.12518941396948	1.12519881883003	1.12521519996600	1.12523972647179
Extrap.	1.1249994(3)	1.249996(3)	1.1249995(2)	1.249997(4)

TABLE XIII. Estimate of the amplitude  $A(\gamma, b)$  in (5.19) for various values of the deformation parameter  $\gamma$  on the self-dual line  $\gamma b = \pi/4$ . Also given is our conjectured value from Eq. (6.17).

$L \setminus \gamma/\pi$	0.45	0.40	0.35	0.30	0.25	0.20	0.15
16	0.172989	0.227420	0.712062	1.34413	2.12657	3.24556	5.21619
32	0.0633073	0.349476	0.901673	1.53538	2.35209	3.54601	5.59051
64	0.0713748	0.473826	0.995320	1.60634	2.42813	3.64798	5.70463
128	0.116176	0.554262	1.03345	1.62997	2.45182	3.68013	5.73713
256	0.181819	0.592325	1.04769	1.63789	2.45947	3.69057	5.74664
512	0.233158	0.607484	1.05292	1.64080	2.46234	3.69445	5.74995
1024	0.258706	0.613073	1.05493	1.64209	2.46371	3.69626	5.75155
2048	0.268682	0.615098	1.05580	1.64278	2.46452	3.69729	5.75262
conject.	5/18	5/8	15/14	5/3	5/2	15/4	35/6